THE EFFECT OF VARIABLE PROPERTIES ON THERMOPHORESIS OF AEROSOL PARTICLES IN TWO-DIMENSIONAL LAMINAR FLOW

by

GHULAM JILANI

DEPARTMENT OF MECHANICAL ENGINEERING

INDIAN INSTITUTE OF TECHNOLOGY KANPUR

MAY 1990

THE EFFECT OF VARIABLE PROPERTIES ON THERMOPHORESIS OF AEROSOL PARTICLES IN TWO-DIMENSIONAL LAMINAR FLOW

A Thesis Submitted
in Partial Fulfilment of the Requirements
for the Degree of

MASTER OF TECHNOLOGY

by

GHULAM JILANI

to the

DEPARTMENT OF MECHANICAL ENGINEERING

INDIAN INSTITUTE OF TECHNOLOGY KANPUR

MAY 1990

C E R T I F I C A T E

It is certified that the work contained in the thesis entitled "The Effect of Variable Properties on Thermophoresis of Aerosol Particles in Two-Dimensional Laminar Flow" by Ghulam Jilani, has been carried out under my supervision and that this work has not been submitted elsewhere for a degree

(Dr. V. Eswaran)
Assistant Professor
Department of Mechanical Engineering
Indian Institute of Technology
Kanpur

May, 1990

A B S T R A C T

Thermophoresis, the drift of sub-micron-sized particles in the direction of decreasing temperature, is of interest in many flows with engineering applications It occurs in situations involving high temperatures and temperature gradients Few researchers have considered the effects of these parameters on the thermophysical properties of the basic flow This thesis incorporates these effects in studying the two-dimensiona subsonic flow over a cold circular cylinder The approach is numerical in nature . finite differenced equations are used to stucy the effects of various parameters on the flow and on the thermophoresis It is found that the predicted velocity temperature, and concentration profiles are significantly changed by the incorporation of variable thermophysical properties in the analysis

A C K N O W L E D G E M E N T

I wish to express my sincere gratefulness to Dr. V. Eswaran for his valuable supervision, able guidance, untiring discussions and constructive criticism along with constant encouragement during the course of this investigation He extended his helping hand by sitting with me and carefully going through the draft of this thesis He has been extremely kind, sympathetic and considerate to me. Without his generosity, this thesis could have not been submitted in time. His timely help at a very crucial point can never be forgotten

I also wish to express my gratitude to **Professor Vijay K. Garg** for giving me the opportunity to work on the problem related to this thesis. The discussion with him proved to be very helpful

In bringing this study to fruition it is a pleasure to acknowledge helpful discussions / or correspondance with **Dr. S. Jayaraj**, Asstt. Professor, R E.C , Calicut.

Thanks are also due to brother **Firoz Alam**, Physics Department, I I T , Kanpur for typing this thesis in a most efficient manner.

I also express my sincere gratitude to my parents for their selfless help and devoted encouragement throughout my educational career

Last but not least, I am grateful to my wife **Gulshan Aara** and my children for showing considerable patience during my stay at this esteemed Institution

Dedicated to my

Parents and Eldest Brother

Who

Sacrified Their Self-interest

For The Sake of Entire Family

* * * * *

LIST OF FIGURES

LIST OF TABLES

LIST OF SYMBOLS

Lower case symbols given in parentheses are the dimensional counter parts of the nondimensional quantities denoted by upper case symbols on the same line

a	Radius of aerosol particles
A_1, B_1, C_1	Constants used in Equation 1 5
C,(c)	Particle concentration per unit mass of gas
C_m	Coefficient of gas kinetic isothermal slip
C_p	Specific heat at constant pressure
C_s	Thermal slip coefficient
C_t	Temperature jump coefficient
D	Brownian diffusion coefficient
k_g	Thermal conductivity of gas
k_p	Thermal conductivity of particle
K_n	Knudsen number (based on particle radius)
K	Thermophoretic coefficient
ℓ	Fluid thickness measured from the surface used for grid adaptation (Equation 3 14)
L	Radius of the circular cylinder
M	Mach number
n	Total number of steps in the Y-direction
N	Particle concentration per unit volume of gas
P,(p)	Absolute pressure
P_r	Prandtl number
R_e	Reynolds number
T,(t)	Absolute temperature

$U,(u)$	Velocity component in the X-direction
$U_s,(u_s)$	Inviscid flow velocity on the body surface
$V,(v)$	Velocity component in the Y-direction
$V_T,(V_t)$	Thermophoretic velocity in the Y-direction
$\vec{w}$	Thermophoretic velocity vector
$X,(x)$	Streamwise coordinate along the body surface
ΔX	Mess size in the X-direction
$Y,(y)$	Transverse coordinate normal to the body surf
ΔY	Mesh size in the Y-direction

Greek Symbols

γ	Ratio of the specific heats
θ	Normalised gas temperature [= $(t - t_\infty)/(tw -$
μ	Dynamic viscosity of the gas
ν	Kinetic viscosity of the gas
ρ	Mass density of the gas
ω	Weight function used in Equation 3 10
ϕ	Angle measured from the stagnation point for flow past a circular cylinder

Subscripts

j	Location in the X-direction
k	Location in the Y-direction
w	Value at the wall
∞	Value in the free stream

Superscripts

'	Value from previous iteration
*	Nondimensional quantity

$U,(u)$	Velocity component in the X-direction
$U_s,(u_s)$	Inviscid flow velocity on the body surface
$V,(v)$	Velocity component in the Y-direction
$V_T,(V_t)$	Thermophoretic velocity in the Y-direction
$\vec{w}$	Thermophoretic velocity vector
$X,(x)$	Streamwise coordinate along the body surface
ΔX	Mess size in the X-direction
$Y,(y)$	Transverse coordinate normal to the body surface
ΔY	Mesh size in the Y-direction

Greek Symbols

γ	Ratio of the specific heats
θ	Normalised gas temperature $[= (t - t_\infty)/(tw - t_\infty)]$
μ	Dynamic viscosity of the gas
ν	Kinetic viscosity of the gas
ρ	Mass density of the gas
ω	Weight function used in Equation 3 10
ϕ	Angle measured from the stagnation point for flow past a circular cylinder

Subscripts

j	Location in the X-direction
k	Location in the Y-direction
w	Value at the wall
∞	Value in the free stream

Superscripts

'	Value from previous iteration
*	Nondimensional quantity

CHAPTER 1

INTRODUCTION

Thermophoresis is the phenomenon by which submicron - sized aerosol particles suspended in non-isothermal gas streams acquire a velocity in the direction opposite to the temperature gradient. This phenomenon causes the particles to migrate from hotter to colder regions of the gas.

The explanation of this phenomenon is based upon kinetic theory arguments, i.e., the particle receives a greater number of molecular impacts on the hotter side than the colder one, thus leading to net rate of change of momentum in the direction opposite to the temperature gradient. The resulting radiometric force experienced by the particles is called the thermophoretic force. This force, like other interactions between particles and gas, depends essentially upon (1) the Knudsen number, K_n (= the ratio of the mean free path, λ of the gas molecules to the particle radius, a and (2) on the ratio of the thermal conductivities of the particles and of surrounding gas. Thermophoresis is of considerable importance for particles having radii as large as 10 μm in fields with temperature gradients of the order of 5K/mm (cf. Walker et al., 1979). A common example of the phenomenon is the blackening of the glass globe of a kerosene lantern; the temperature gradient established between the flame and the globe drives the carbon particles produced in the combustion process towards the globe, where they deposit. Thermophoresis also causes the dirt pattern on

the ceiling of kitchens

The phenomenon of thermophoresis is of technical importance as is discussed in detail by Green and Lane (1964) and Fuchs (1964). There are numerous technological and environmental problems which involve deposition of aerosol particles. Of current concern is the deposition of radioactive aerosol particles inside a nuclear reactor containment following a hypothetical accident, this plays a critical role in reducing the amount of radioactivity that might subsequently escape to the atmosphere

Thermophoresis has also been cited as a cause for the deposition of particulate matter on heat exchange surfaces with the attendant reduction of the heat transfer co-efficient. Due to the sharply increasing cost of high-grade fuels, there is renewed interest in the combustion of coal- derived or lower grade 'residual' petroleum - derived gas turbine fuels containing inorganic impurities. At the same time, there is a need for higher turbine inlet temperature to raise thermodynamic efficiency. However, the metal temperature is limited by structural considerations and is maintained by film or transpiration cooling etc As a result, the high temperature gradients, and the large concentration of contaminants (ash, salts) present in the combustion products of lower grade fuels, leads to the formation and possible deposition of particles on gas turbine blade surfaces giving rise to highly accelerated blade corrosion and /or fouling rate. Hence, blade surfaces lose aerodynamic efficiency even if the changes in shape are small. Under these

combined circumstances, thermophoresis plays an important role in determining mass deposition rates as demonstrated by Goren (1977) and by Gokoglu and Rosner (1986) Such results and techniques are also necessary to develop systems for "clean" hydrocarbon fuels combustion since 1) local fuel pyrolysis and inadequate oxidation rates can cause soot particles production and deposition, and/or 2) the air ingested for combustion may itself contain inorganic substances (e g , dust), which can deposit on gas-turbine components.

Thermophoresis is also of practical use in removing aerosol particles like dust, mist, smoke etc from air in a room or from gas streams in various channels The thermal precipitator is one such piece of equipment, designed to utilize this phenomenon positively It is sometimes more effective than electrostatic precipitators in removing submicron - sized particles from gas streams (Talbot et al., 1980). It is particularly effective in removing small particles with a diameter a micron or less Other important application of thermophoresis are in determining exhaust gas trajectories from combustion devices, in the manufacture of fumed silica, carbon black, and titania particles for paint industry, in the design of aerosol sampling devices, in chemical coating of metals, etc It has also been demonstrated recently that thermophoresis is the dominant mass transfer mechanism in the Modified Chemical Vapour Deposition (MCVD) and Outside Vapour Deposition (OVD) processes employed in the fabrication of optical fiber preforms (Simpkins et al., 1979; Walker et al , 1980, Alam and Mehrotra, 1987) It is

by now apparent that silicon based optical fibers having low loss and wide band width are in the process of revolutionizing the technology of communications by replacing conventional copper cables

The fact that scrubbing in aerosol scrubbers is more effective when the dusty air is preheated has been ascribed to thermophoresis The reverse effect, namely, the repulsion of particles from a hot wall and the formation of the "dust- free" regions in the vicinity of hot walls, has also been observed Because such "clean" layers shield hot surfaces from particles in tne environment, the phenomenon has recently been recognised as an efficient means to protect electronic components from particle deposition during their manufacturing.

1 1 Literature Review

The basic physical processes involved in the phenomenon of thermophoresis were first investigated by Maxwell (cf. Kennard,1938), in an attempt to explain the radio-metric effect. Subsequently, this phenomenon has been the subject of theoretical and experimental studies by a variety of investigators. The extensive literature on these investigations contains a number of conflicting results. A brief review of the existing important literature follows below :

1.1.1 Thermophoretic Coefficient

Small particles suspended in gas streams containing a temperature gradient are known to be subjected to the thermophoretic

force and move steadily from hotter to colder regions in balance with viscous drag As a consequence, the velocity acquired by the particles relative to the gas is known as the thermophoretic velocity Theoretical analyses yield the following linear relation between the thermophoretic velocity, $\vec{w}_t$ of a particle and the local temperature gradient, ∇t

$$\vec{w}_t = - K \frac{\nu}{t} \nabla t \qquad (1.1)$$

where t is ambient absolute temperature of the gas, ν is the kinematic viscosity of the gas, and K the dimensionless thermophoretic coefficient This coefficient is an important parameter in the particle transport and deposition The value of the thermophoretic coefficient depends mainly on the regime of flow as well as on the ratio of thermal conductivities of the particle and gas For free molecular flow ($K_n >> 1$), Waldmann found the coefficient to be 6/8 when there are elastic collisions of the molecules with the aerosol particles, and 6/(8 + π) for collisions resulting in condensation and reevaporation (cf Goren, 1977) For the slip flow regime ($K_n << 1$) Epstein was first to calculate the thermophoretic velocity by solving the equation of viscous hydrodynamics (cf. Derjaguin et al , 1976). With an arbitrary value of thermal slip coefficient, C_s = 0.75, the Epstein's formula for thermophoretic coefficient is

$$K = C_s \frac{k_g}{k_g + k_p/2} \qquad (1 2)$$

where k_g and k_p are the thermal conductivities of the gas and the particles, respectively Brock (1962) made the formula more precise to the technologically important transition range where the mean free path, λ is of the order of the particle radius, a His formula for K is

$$K = C_s \frac{1 + C_t \lambda/a \; k_p/k_g}{(1 + k_p/2k_g + C_t \lambda/a \; k_p/k_g)(1 + 2C_m \lambda/a)} \qquad (1\ 3)$$

where C_t, C_m are temperature jump coefficient and velocity jump coefficient, respectively and have values C_t = 2 16, C_m = 1 23 Brock's result, with C_s = 0 75, is found to be not in good agreement with experiment for particles of high thermal conductivity, although the discrepancy is much less than that obtained using the Epstein result

An expression for calculating the thermophoretic coefficient has been proposed by Derjaguin et al (1976) The thermophoretic velocities measured by them support the expression

$$K = C_s \frac{(1 + C_t \lambda/a \cdot k_p/k_g)}{(1 + k_p/2_g + C_t \cdot \lambda/a \; k_p/k_g)} \qquad (1\ 4)$$

where C_s= 1 1, close to theoretical value and C_t= 2 17. Equation (1.4) is the formula most frequently cited in the current literature But because of the questionable nature of the theory underlying this result, plus the adjustment of the constant, it can hardly be regarded as more than an empirical formula.

More recently, a critical review of the data and theore-

tical expressions for thermophoretic coefficient has been given by Talbot et al. (1980) They give evidence in support of their belief that the following expression for K is tolerably accurate for all regimes from free molecular flow to continuum flow:

$$K = 2\,C_s\,\frac{(k_g/k_p + C_t\ \lambda/a)\,[1 + \lambda/a\,(A_1 + B_1 e^{-C_1\ a/\lambda})\,]}{(1 + 3\,C_m\ \lambda/a)\,(1 + 2\,k_g/k_p + 2\,C_t\,\lambda/a)} \qquad (1.5)$$

in which the constants have the values $A_1 = 1\ 20$, $B_1 = 0.41$, $C_1 = 0\ 88$, $C_s = 1\ 17$, $C_t = 2\ 18$ and $C_m = 1\ 14$ The semiempirical relation (1 5) appears reasonably satisfactory for the entire range, $0 \leq K_n \leq \infty$. However, accurate measurement of K is difficult and the agreement between the available data and the theoretical values is not close Nevertheless, in most of the literature reviewed in section 1 1 2, it was contended that K can be treated as a specified constant of order 1 and independent of temperature in the flow field.

1.1 2 Thermophoretic Flow Investigations

Thermophoretic deposition of aerosol particles in flow fields have been the subject of many investigations. Laminar thermophoretic flow over a flat plate at zero incidence was analysed theoretically in detail by Goren (1977) for both cold and hot walls. Compressibility effects were retained because thermophoresis frequently occurs under large temperature differences for which the fluid properties may vary. The governing boundary layers equations were transformed to forms suitable

for solution by invoking Howarth -Doridnitsyn transformation. The similarity solutions with and without viscous dissipation were obtained in the absence of Brownian diffusion whose effect is only to form a very thin sublayer even on the boundary layer scale For cold walls, the particle concentration drops monotonically as the wall is approached and a finite concentration at the wall is found depending upon the wall temperature For hot walls, the presence of a critical layer within the concentration boundary layer is indicated by Goren He also emphasized the importance of the factor P_rK in determining the concentration profile over a hot wall, where P_r is the Prandtl number The effect of viscous dissipation on particle concentration profile, exhibited for cold wall conditions,indicates that wall particle concentration reduces with increasing dissipation rates

Thermophoretic deposition of small particles in laminar incompressible flow through a tube with a prescribed wall temperature distribution has been studied theoretically by Walker et al. (1979) who included the effects of Brownian diffusion by the use of matched asymptotic expansions They found that only a fraction of the particles present initially in the stream get deposited on the cold tube wall. This was because of the ultimate relaxation of the temperature gradient far downstream. It is evident that their similarity solution is valid only within a short axial distance from the start of the constant wall temperature. This solution was extended downstream using numerical methods It was also observed that cumulative

efficiency rapidly approaches an asymptotic limit for any wall temperature and $P_r K$ value (along the axial direction)

An analytical study of thermophoretic deposition of small particles was carried out by Homsy et al. (1981) This was the first investigation which dealt with an external flow in the presence of a non-zero pressure gradient. Their analysis was based on the development of thermophoretic flux in terms of Blasius series The values of particle flux coefficient were calculated numerically as functions of K and wall temperature for fixed Prandtl number, P_r= 0 71 Knowing the outer potential flow constants, one can obtain the corresponding deposition profile from these particle flux coefficients The local depositions profile plotted for transverse flow past a circular cylinder as an illustrative example, exhibits maximum deposition rate of the stagnation point and zero near the cylinder angle, ϕ = 90° For still larger ϕ physically impossible negative values result because the truncated Blasius series is not accurate The total deposition rate was found to decrease monotonically with increasing wall temperature.

Thermophoretic transport of small particles through both laminar and turbulent natural convection boundary layers adjacent to cold vertical plates have been analysed by Epstein et al. (1985). Introducing conventional Pohlhausen similarity transformation, the governing boundary layer equations are reduced to ordinary differential equations by exploiting the concept of local similarity. Numerical solutions of these equations have been obtained with P_r, K and tw/t_∞ as

parameters Dimensionless particle concentrations at the wall as a function of K, for P_r = 0 73, have been plotted for laminar flow It is evident from this graph that the wall particle concentration decreases with decreasing tw/t_∞ and increasing K Interestingly enough, it is noted that while the particle concentration distribution for laminar flow differs distinguishable in shape from that for turbulent flow, at the wall two profiles converges to practically the same particale concentration

A detailed theoretical analysis of thermophoretic deposition of particles on a cold surface has been presented by Batchelor and Shen (1985) By neglecting viscous dissipation and Brownian diffusion, a few exact relations are derived which are of general application to different flow fields These relations suggest that the dimensionless wall particle concentration Nw/N_∞ is approximately uniform over a cold isothermal boundary (at wall temperature, tw), that the total particle flux to the boundary is proportional to the total heat flux to the boundary, and that the relation between Nw/N_∞ and tw/t_∞ is approximately the same for all flow systems These results are further compared with the available numerical results for a number of steady flow systems and found to be in good agreement except when both tw/t_∞ and K are small

Thermophoresis of aerosol particles in two-dimensional laminar flow in the presence of non-zero pressure gradient has been analysed in detail by Jayaraj (1988) The boundary layer-type governing equations are solved using a simple finite-

difference marching technique for cold, hot and adiabatic wall conditions. While a non-uniform grid is used in the marching direction, the grid size in the transverse direction is self-adapted Results are presented for flow over an inclined plate and a circular cylinder for different values of t_w/t_∞ keeping P_r and K as constant Irrespective of the geometry of flow, the particle concentration at the cold wall is found to be almost independent of location and also of the angle of inclination (of the inclined plate). For both the inclined plate and the circular cylinder, the thickness of the critical layer increases as one moves away from the stagnation point The influence of viscous dissipation on the particle concentration is also discussed

Quite recently, the thermophoretic deposition of small particles on cold surfaces has been treated by Shen (1989). He investigates the external flow problem and proposes a general method of calculating the thermophoretic deposition rate of particles suspended in two-dimensional or axisymmetric flow past a body which is held at a lower temperature than the flow. Special consideration is given to the flow near the stagnation-points of a cylinder and a sphere, and the flow past a flat plate to show explicitly how the wall particle concentration, c_w/c_∞ and deposition rate are influenced by the density variations. A general numerical procedure for this problem is used for calculations of the thermophoretic deposition of particles in flows past a cold cylinder and a cold sphere. Results for c_w/c_∞ at the stagnation point of the cylinder indicate that

this quantity decreases with decreasing t_w/t_∞ and increasing $P_r K$ It is also seen, for a range of values of $P_r K$ and t_w/t_∞, that c_w/c_∞ remains almost constant along the surface This last result is also true for the flow over a sphere

1.2 Objective of Present Investigation

Very few investigators to date have considered the effect of gas thermophysical property variations in the analysis of thermophoresis Only Goren (1977) and Shen (1989) took into account the effect of density variation on the thermophoretic deposition Goren treated the thermophoresis of aerosol particles in the laminar, compressible, boundary layer flow past a flat plate by using similarity transformations However, most of the practical applications of thermophoresis in external flow involve a non-zero pressure gradient (either due to the shape of the body or due to its orientation with respect to the main flow) for which no similarity solution is possible

Shen studied thermophoretic deposition of small particles onto cold surfaces of bodies in two-dimensional and axisymmetric flows He included the compressibility effects with the assumption that the product $\mu\rho$ is a constant where, μ is the dynamic viscosity and ρ, the density of the gas. (This assumption was made by Goren as well) This is a well-known simplification and is close to reality for not-too-large variations in temperature. However, it should be emphasized here that thermophoresis is frequently found under conditions of large temperature gradients. Thus, the application of above assumption may lead to erroneous results. In addition to this assumption, Shen

neglects the effect of viscous dissipation by taking $M_\infty^2 << 1$ which excludes most of the thermophoretic flows of engineering interest For example, current combustion turbine blades experience high subsonic Mach numbers say, $M_\infty = 0.8$ (cf Gokoglu and Rosner, 1986) It is well-known that viscous dissipation modifies temperature profiles in momentum diffusion boundary layer Therefore, the assumption of no viscous dissipation will give inaccurate results There have been relatively few investigations in which the effect of viscous dissipation is included Moreover, Shen analysed the flow past circular cylinder by assuming inviscid, incompressible flow outside the boundary layer which differs very much from the real outer flow except for low Mach numbers

The objective of the present work is to study the effect of variable thermophysical properties on velocity, temperature and concentration profiles with special reference to thermophoretic deposition Accordingly, a pressure distribution is imposed on the laminar compressible boundary layer over a cold cylinder The pressure gradient is known from inviscid flow solution in the free stream The governing partial differential equations are solved by an implicit finite difference marching technique; while prespecified variable mesh size is used in the marching direction, the grid size in the transverse direction is self-adapted. The numerical solution includes the effect of viscous dissipation and neglects Brownian - diffusion (which influences only an extremely thin layer near the wall)

CHAPTER 2

MATHEMATICAL FORMULATION

The first step in assessing the quantitative importance of thermophoretic deposition of aerosol particles is to develop a mathematical model of the flow systems under consideration The actual flow fields encountered in most of the thermophoretic applications are of a very complex nature The non-zero pressure gradient in the boundary layer over a body, common in these applications, is due to either the shape of the body or to its orientation with respect to the undisturbed flow This pressure gradient causes further complications Certain idealizations of the physical model need to be made before a mathematical model can be obtained In this chapter, the governing equations for thermophoretic flow past a cold circular cylinder will be analysed

2 1 Physical Model

Consider a stream of hot gas, containing suspended aerosol particles, flowing past a circular cylinder maintained at a lower temperature than that of the oncoming stream [see Figure (2.1)] The temperature gradient established in the forward moving forced-convection boundary layer between the surface of the cylinder and the gas-particle mixture drives the particles towards the surface, where they deposit. Here, we consider the case of two-dimensional subsonic flow with significant Mach number effects.

The particle concentration is assumed to be sufficiently

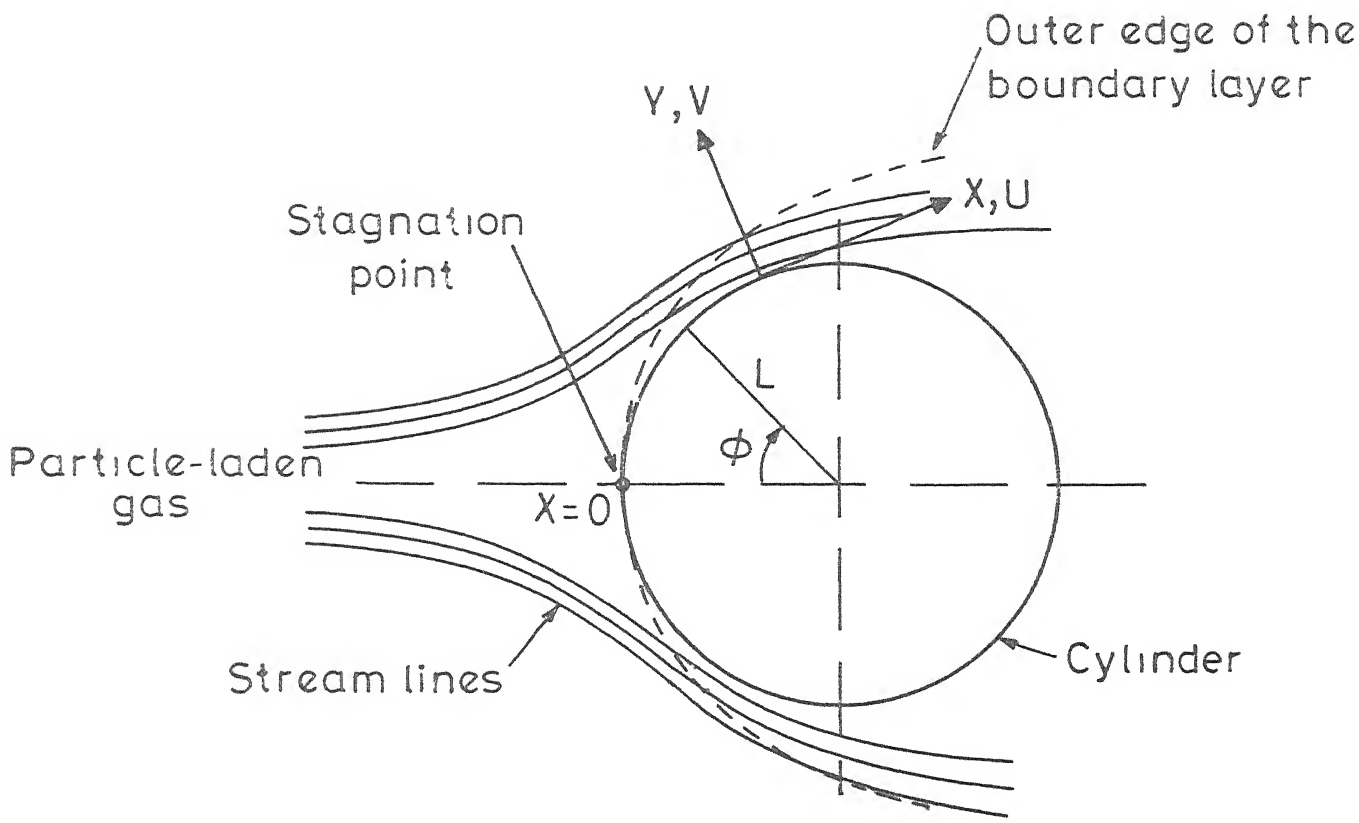

Figure 2·1 Flow past a Circular Cylinder

dilute so that the velocity and temperature profiles of the gas can be determined as in a flow free of particles and the thermophysical properties of the mixture are those of the gas-phase For particles of unit density, (i e., particle mass density comparable to that of the gas) and 1 μm radius, this assumptions limits the analysis to aerosol concentration less than about 10^7 particles per cubic centimeter of the gas (Goren, 1977) This is indeed the case for most of the thermophoretic applications Additional assumptions usually made for the idealization of a physical model in thermophoretic analysis (Goren, 1977, Walker et al , 1979; Epstein et al, 1985) are :

(i) The particles are small enough so that in the absence of thermophoresis, the particle moves with the local gas velocity

(ii) Thermophoretic velocity component in the streamwise direction is negligible

(iii) The effect of Brownian diffusion is restricted only to an extremely thin layer next to the surface

(iv) The effect of thermal radiation is negligible (This excludes the case of absorbing aerosols

In addition, the thermophysical properties of the gas are assumed to be functions of temperature alone.

2.2 Governing Equations

The boundary layer equations governing the velocity and temperature fields have been thoroughly reviewed (White, 1974, Schreier, 1982; Schlichting, 1979). For a steady, laminar,

two-dimensional, compressible flow with variable thermophysical properties, these equations are (Schlichting, 1979) .

Total mass $$\frac{\partial (\rho u)}{\partial x} + \frac{\partial (\rho v)}{\partial y} = 0 \qquad (2.1)$$

Streamwise momentum :

$$\rho \left(u \frac{\partial u}{\partial x} + v \frac{\partial u}{\partial y} \right) = - \frac{dp}{dx} + \frac{\partial}{\partial y} \left(\mu \frac{\partial u}{\partial y} \right) \qquad (2.2)$$

Energy

$$\rho C_p \left(u \frac{\partial t}{\partial x} + v \frac{\partial t}{\partial y} \right) = u \frac{dp}{dx} + \frac{\partial}{\partial y} \left(k_g \frac{\partial t}{\partial y} \right) + \mu \left(\frac{\partial u}{\partial y} \right)^2 \qquad (2.3)$$

where, (u,v) are velocity components in (x,y) directions [see Figure (2.1)], ρ, p and t are, respectively, the density, pressure and temperature of the gas, and ρ, C_p and k_g are the dynamic viscosity, specific heat at constant pressure, and thermal conductivity of the gas

In the equations (2.2) and (2.3) the local pressure field is assumed to vary only in the streamwise direction, i.e., pressure remains a constant across the boundary layer and is given by the inviscid flow solution More details will be given in Section 2.3

The equation system (2.1) to (2.3) is mixed parabolic/hyperbolic and, consequently, requires the following boundary conditions.

$$
\begin{aligned}
u\,(x,\,0) &= 0 \quad , \\
v\,(x,\,0) &= 0 \quad , \\
u\,(x,\,\infty) &= u_s(x) \quad , \\
u\,(0,\,y) &= u_s(0) \quad , \\
t\,(x,\,0) &= t_w \quad \text{for isothermal wall,} \\
t\,(x,\,\infty) &= t_\infty \quad , \\
t\,(0,\,y) &= t_\infty \quad ,
\end{aligned} \tag{2.4}
$$

where t_∞ is the free stream temperature, t_w, the surface temperature and $u_s(x)$ is inviscid flow velocity at the body surface

It should be pointed out that the boundary layer equations are really not valid at $x = 0$ In computation, the effect of the singularity at the stagnation point is handled by selecting a very small step size in the x-direction (Hornbeck, 1973)

Due to the boundary layer behaviour, the temperature gradient, $\frac{\partial t}{\partial y}$ in the direction normal to the surface is very much larger than in the tangential direction, $\frac{\partial t}{\partial x}$. Also, the gas velocity component, u in the tangential direction is large compared to v, the gas velocity component in the normal direction This implies that the normal thermophoretic velocity components, v_t, only needs to be considered. Using equation (1.1), v_t is given by

$$
v_t = -K \frac{\nu}{t} \frac{\partial t}{\partial y} \tag{2.5}
$$

As mentioned in section 1.1 1, Talbot et al. (1980) proposed a semiempirical formula for K which seems to be accurate for a wide range of Knudsen numbers. However, in most of the thermo-

phoretic calculation K is usually taken as a constant in the range of 0.2 to 1 2 For the present study, K is assumed as specified constant

For compressible flow it is more convenient to introduce c, the particle concentration per unit mass of gas The particle concentration per unit volume, N and c are related by

$$c = N/\rho \tag{2.6}$$

where ρ is the density of the carrier gas

With the usual boundary layer approximation, the species mass conservation equation for the physical model depicted in section 2.1 can be written as

$$\frac{\partial}{\partial x}(\rho cu) + \frac{\partial}{\partial y}[\rho c(v + v_t)] = \frac{\partial}{\partial y}[D\frac{\partial(\rho c)}{\partial y}] \tag{2.7}$$

where, D is the Brownian diffusivity of the particles. Equation (2.7) can be rewritten in simplified form using the total mass conservation equation (2 1) as

$$\rho u\frac{\partial c}{\partial x} + \rho v\frac{\partial c}{\partial y} + \frac{\partial}{\partial y}(\rho c v_t) = \frac{\partial}{\partial y}[D\frac{\partial}{\partial y}(\rho c)] \tag{2.8}$$

The boundary conditions are

$$c(0, y) = c_\infty \quad ,$$

$$c(x, \infty) = c_\infty \quad ,$$

$$\text{and} \qquad c(x, 0) = 0 \tag{2.9}$$

if the wall is totally absorbing Here, c_∞ is the particle concentration in the free stream

The Brownian diffusivity, D, of aerosol particles of diameter 0 05-1 0 μm is very much smaller than any of the gas diffusivities (for mass, momentum, heat). For example, for particles with a size of 0 1 μm the particle Brownian diffusivity is of the order of $10^{-5} cm^2 s^{-1}$ Thus, for particle of this size or larger the Brownian diffusion sublayer is so thin even in comparison with the boundary layer thickness that it does not affect the thermophoretic deposition rate (Goren, 1977; Walker et al., 1979) The only effect of Brownian diffusion is to create a thin particle concentration boundary layer adjacent to the cold surface. Hence, the particle diffusion term on the right- hand side of Equation (2 8) could be dropped and can be rewritten as

$$\rho u \frac{\partial c}{\partial x} + \rho v \frac{\partial c}{\partial y} + \frac{\partial}{\partial y} (\rho c v_t) = 0 \qquad (2.10)$$

Equation (2 10) is of the first order in y. It implies that only one y-boundary condition (at infinity) will be needed for its solution. In the absence of diffusion, a finite particle concentration at the wall is expected for the cold wall condition. This wall particle concentration may be obtained by solving Equation (2 10). In fact, this concentration corresponds to the outer edge of the very thin Brownian diffusion sublayer adjacent to the cold surface.

2 3 Pressure Distribution

The calculation of the pressure gradient in the boundary layer is essential for the solution of the momentum and energy equations The pressure and velocity distribution at the wall are calculated on the basis of inviscid flow theory and then used as conditions at the outer edge of the boundary layer. Since the thickness of the boundary layer is not known a priori, the conditions are applied at $y = \infty$ in the solution In short, the condition at $y = 0$ for inviscid flow are assumed to prevail at $y = \infty$ in the viscous flow problem. This procedure is, of course, widely used in Fluid Mechanics, its justification being that it is found to give good results in thin boundary layers Solutions found in this way show that the velocity reaches 99% of its inviscid value at a short distance from the wall, thus confirming to the boundary layer concept The pressure in the boundary layer is found from (Schreier, 1982)

$$-\frac{1}{\rho}\frac{dp}{dx} = u_s \frac{d u_s}{dx} \qquad (2.11)$$

The pressure gradient, $\frac{dp}{dx}$ is usually computed by considering inviscid flow over the body surface Two-dimensional, inviscid, compressible, subsonic flow over a circular cylinder is assumed to be uniform at infinite with zero strength and zero circulation. The following expression for dimensionless velocity over the circular cylinder is obtained by the Rayleigh - Janzen method (Schreier, 1982)

$$u_s = \frac{u_\infty}{3} \sin\left(\frac{x}{L}\right)\left[\left(6 + \frac{7}{2} M_\infty^2\right) - 6 M_\infty^2 \cos^2\left(\frac{x}{L}\right)\right] \qquad (2.12)$$

where L is the radius of the cylinder and x corresponds to the location on the cylinder surface from the stagnation point The equation (2.11) can be rewritten with the help of equation (2.12) as

$$-\frac{1}{\rho}\frac{dp}{dx} = \frac{u_\infty^2}{3L} \sin\left(\frac{x}{L}\right)\cos\left(\frac{x}{L}\right)\left[\left(6 + \frac{7}{2} M_\infty^2\right) - 6 M_\infty^2 \cos^2\left(\frac{x}{L}\right)\right] .$$

$$\left[2 + \frac{31}{6} M_\infty^2\right) - 6 M_\infty^2 \cos^2 (x/L) \qquad (2.13)$$

2.4 Constitutive Relations

There are only six equations in nine unknown variables, that is u, v, v_t, p, t, c, ρ, μ, and k_g In order to solve these equations, three more constitutive equations of state will be necessary. One such well-known constitutive equation is equation of state for perfect gas, i.e.,

$$p = \rho R t \qquad (2.14)$$

The dynamic viscosity, μ, and thermal conductivity, k_g of the gas are generally assumed to be functions of temperature only. The commonly employed power-law relationship will be used here. These expressions for μ and k_g are (cf. Gokoglu and Rosner, 1986) :

$$\mu/\mu_\infty = \left(\frac{t}{t_\infty}\right)^{0.70} \qquad (2.15)$$

$$k_g / k_{g\infty} = \left(\frac{t}{t_\infty} \right)^{0.85} \qquad (2.16)$$

where μ_∞ and $k_{g\infty}$ are the values at the stream temperature t_∞

2.5 Dimensionless Representation

The dimensionless form of system of equation are more compact and have less steep velocity, temperature and concentration gradients The sharp gradients usually create convergence problems in numerical calculations In addition, nondimensionalising of the governing equations leads to the identification of nondimensional numbers based on which the result can be predicted Following dimensionless variable are introduced

$$X = \frac{x}{L} ,$$

$$Y = (y/L) R_{e_\infty}^{1/2} ,$$

$$U = \frac{u}{u_\infty} ,$$

$$V = \left(\frac{v}{u_\infty} \right) R_{e_\infty}^{1/2} ,$$

$$T = \frac{t}{t_\infty} ,$$

$$P = \frac{p - p_\infty}{\rho_\infty u_\infty^2} ,$$

$$\rho^* = \rho/\rho_\infty ,$$

$$V_T = v_t (L/\nu_\infty) R_{e_\infty}^{-1/2} \quad ; \quad \nu_\infty = \mu_\infty/\rho_\infty$$

$$C = \frac{c}{c_\infty} ,$$

$$\mu^* = \mu/\mu_\infty ,$$

$$K_g^* = K_g/K_{g\infty} ,$$

and $$U_s = \frac{u_s}{u_\infty} \qquad (2.17)$$

Here, L is the radius of the circular cylinder and R_{e_∞} is the free stream Reynolds number defined as

$$R_e = \frac{u_\infty L}{\nu_\infty} \tag{2.18}$$

In addition, the following nondimensional numbers are introduced in the energy equation :

$$\text{Prandtl number} \quad , \quad P_r = \frac{\mu_\infty C_p}{K_{g_\infty}} \quad , \quad C_p = \frac{\gamma R}{\gamma - 1}$$

$$\text{Mach number} \quad , \quad M_\infty = u_\infty / (\gamma R t_\infty)^{1/2} \tag{2.19}$$

where, γ is the specific heat ratio and R, the gas constant.

Using above dimensionless variables and nondimensional numbers, the system of Equations (2.1) to (2.5) and (2.9) to (2.16) can be rewritten in dimensionless form as given below :

Total mass conservation :

$$\frac{\partial (\rho^* U)}{\partial X} + \frac{\partial (\rho^* V)}{\partial Y} = 0 \tag{2.20}$$

Streamwise momentum :

$$\rho^* \left(U \frac{\partial U}{\partial X} + V \frac{\partial U}{\partial Y}\right) = - \frac{dP}{dX} + \frac{\partial}{\partial Y} \left(\mu^* \frac{\partial U}{\partial Y}\right) \tag{2.21}$$

Energy :

$$\rho^* \left(U \frac{\partial T}{\partial X} + V \frac{\partial T}{\partial Y}\right) = (\gamma - 1) M_\infty^2 U \frac{dP}{dX} + \frac{1}{P_r} \frac{\partial}{\partial Y} \left(k_g^* \frac{\partial T}{\partial Y}\right) +$$

$$(\gamma - 1) M_\infty^2 \mu^* \left(\frac{\partial U}{\partial Y}\right)^2 \tag{2.22}$$

Euler's equation

$$-\frac{1}{\rho^*}\frac{\partial P}{\partial X} = U_s \frac{dU_s}{dX} \qquad (2\ 23)$$

Thermal boundary velocity

$$V_T = -\frac{\nu^*}{T}\frac{\partial T}{\partial Y}, \quad \nu^* = \frac{\mu^*}{\rho^*} \qquad (2.24)$$

Species mass

$$\rho^* \left(-\frac{\partial C}{\partial X} + V\frac{\partial C}{\partial Y}\right) + \frac{\partial}{\partial Y}(\rho^* C V_T) = 0 \qquad (2\ 25)$$

Constitutive Equations

$$\rho^* = (T)^{-1\ 0} \qquad (2.26)$$

$$\mu^* = (T)^{0\ 70} \qquad (2\ 27)$$

$$k_g^* = (T)^{0\ 85} \qquad (2\ 28)$$

The boundary conditions .

$$U(X, 0) = 0 ,$$

$$V(X, 0) = 0 ,$$

$$U(X, \infty) = U_s(X) ,$$

$$U(0, Y) = U_s(0) ,$$

$$T(X, 0) = T_w \quad \text{(isothermal wall)},$$

$$T(X, \infty) = 1 ,$$

$$T(0, Y) = 1 ,$$

$$C(X, \infty) = 1 ,$$

and $$C(0, Y) = 1 \qquad (2.29)$$

2.6 Strategy for Solution

The governing equations (2.1) to (2.3) and (2.10) are nonlinear coupled partial differential equations. They are so complicated that an analytical solution especially in the presence of non-zero pressure gradient is not only difficult but probably impossible. Hence it is essential to seek a numerical solution to these equation.

The solution to these system of equation can be obtained using the finite-difference technique while marching in the x-direction. The pressure gradient required for the solution of momentum and energy equation can be computed by inviscid compressible flow considerations. Both streamwise momentum and total mass conservation equations can be solved simultaneously in an iterative manner to arrive at the correct velocity profiles. Once the two velocity components are known, the temperature profile can be obtained by solving the energy equation. Finally, the particle concentration equation can be solved using the known values of density and dynamic viscosity at the current location.

CHAPTER 3

COMPUTATIONAL TECHNIQUE

The process of obtaining the computational solution consists of two stages The first stage converts the continuous partial differential equations and auxiliary (boundary and initial) conditions into a discrete system of algebraic equations This stage is called 'discretisation' The second stage requires an 'equation solver' to provide the solution of the system of algebraic equations

A number of choices are available for the discretisation of the governing partial differential equations · the finite-difference method, the finite-element method and the spectral method The finite-difference method is used here The finite-difference method consists of the construction of a discrete grid, the replacement of the continuous derivatives in the governing partial differential equations with equivalent finite-difference expressions and the solution of the resulting algebraic equations by an algorithm This chapter is concerned with the computational techniques for obtaining and solving the system of algebraic equations generated from the governing equations (2 20) to (2.25).

3 1 Discretisation of the Governing Equations

In local methods, like the finite-difference method, the discretised algebraic equations link together values of the dependent variables at adjacent grid points In order to convert the dimensionless differential equation (2.20) to (2.25)

In finite difference form, a two-dimensional rectangular mesh is superimposed on the flow field over the circular cylinder. Indices (j,k) are used to indicate the position of a point in the boundary layer corresponding to $X = \sum_{i=1}^{j} \Delta X_i$ and $Y = \sum_{i=1}^{j} \Delta Y_j$ (j, k are integers greater than 0), where ΔX_i and ΔY_i are grid intervals. That is, (0,0) represents the stagnation point both in terms of spatial coordinates and finite-difference indices. The cylinder surface is represented by k = 0 and the edge of the boundary layer by k = n+1.

Because the governing equations are of mixed hyperbolic/parabolic type, the computation can be carried out by "marching" forward in the X-direction. The momentum, energy and concentration equations are solved implicitly at every step. The total mass conservation equation is solved simultaneously with the momentum equation by an iterative algorithm. Forward differencing in the X-direction and the central differencing in the Y-direction are used in Equations (2.21) and (2.22). Forward differencing is employed in Equations (2.20) and (2.24). The finite-difference form of these equations, in a form readily adaptable for solution, is given below .

Total mass conservation equation :

$$V_{J+1,k+1} = \frac{\rho^*_{J+1,k}}{\rho^*_{J+1,k+1}} V_{J+1,k} + \frac{\Delta Y}{\Delta X} \left[-U_{J+1,k+1} + \frac{\rho^*_{J,k+1}}{\rho^*_{J+1,k+1}} U_{J,k+1} \right] \tag{3.1}$$

Streamwise Momentum Equation

$$\left[-\frac{V'_{J+1,k}}{2\Delta Y} - \frac{\mu^*_{J+1,k}}{\rho^*_{J+1,k}(\Delta Y)^2} + \frac{\mu^*_{J+1,k+1} - \mu^*_{J+1,k-1}}{\rho^*_{J+1,k} \cdot 4(\Delta Y)^2} \right] U_{J+1,k-1} +$$

$$\left[\frac{U'_{J+1,k}}{\Delta X} + \frac{2\mu^*_{J+1,k}}{\rho^*_{J+1,k}(\Delta Y)^2} \right] U_{J+1,k} + \left[\frac{V'_{J+1,k}}{2\Delta Y} - \frac{\mu^*_{J+1,k}}{\rho^*_{J+1,k}(\Delta Y)^2} \right.$$

$$\left. - \frac{\mu^*_{J+1,k+1} - \mu^*_{J+1,k-1}}{\rho^*_{J+1,k} \cdot 4(\Delta Y)^2} \right] U_{J+1,k+1} = \frac{U'_{J+1,k}}{\Delta X} U_{J,k} +$$

$$\left(-\frac{1}{\rho^*} \frac{dP}{dX} \right) \quad (3.2)$$

Energy Equation

$$\left[-\frac{V_{J+1,k}}{2\Delta Y} - \frac{k^*_{gJ+1,k}}{\rho^*_{J+1,k}} \frac{1}{P_r(\Delta Y)^2} + \frac{k^*_{gJ+1,k+1} - k^*_{gJ+1,k-1}}{\rho^*_{J+1,k} \cdot 4 P_r (\Delta Y)^2} \right].$$

$$T_{J+1,k-1} + \left[\frac{U_{J+1,k}}{\Delta X} + \frac{2k^*_{gJ+1,k}}{\rho^*_{J+1,k}} \frac{1}{P_r(\Delta Y)^2} \right] T_{J+1,k} +$$

$$\left[\frac{V_{J+1,k}}{2\Delta Y} - \frac{k^*_{gJ+1,k}}{\rho^*_{J+1,k}} \frac{1}{P_r(\Delta Y)^2} - \frac{k^*_{gJ+1,k+1} - k^*_{gJ+1,k-1}}{\rho^*_{J+1,k} \cdot 4 P_r (\Delta Y)^2} \right]$$

$$T_{J+1,k+1} = \frac{U_{J+1,k}}{\Delta X} T_{J,k} - (\gamma - 1) M_\infty^2 U_{J+1,k} \left(-\frac{1}{\rho^*} \frac{dP}{dX} \right) +$$

$$(\gamma - 1) M_\infty^2 \frac{\mu^*_{J+1,k}}{\rho^*_{J+1,k}} \left[\frac{U_{J+1,k+1} - U_{J+1,k-1}}{2\Delta Y} \right]^2 \quad (3.3)$$

Thermophoretic Velocity :

$$V_{T\ j+1,k} = - K \frac{\mu^*_{j+1,k}}{\rho^*_{j+1,k} T_{j+1,k}} \cdot \left[\frac{T_{j+1,k+1} - T_{j+1,k}}{\Delta Y} \right] \qquad (3.4)$$

Constitutive Relations :

$$\rho^*_{j+1,k} = \left(T_{j+1,k} \right)^{-1.0} \qquad (3.5)$$

$$\mu^*_{j+1,k} = \left(T_{j+1,k} \right)^{0.70} \qquad (3.6)$$

$$k^*_{g\ j+1,k} = \left(T_{j+1,k} \right)^{0.85} \qquad (3.7)$$

The above discretisation is second order accurate in Y for U and T.

In order to satisfy the sufficient conditions for a meaningful solution of a triadiagonal set of equations (Roache, 1982) different discretisation forms are used for species mass conservation equations (2.25) depending upon the signs of V. These equations are given below :

Particle Concentration Equation :

Cold wall (V > 0) :

$$- \frac{V_{j+1,k}}{\Delta Y} C_{j+1,k-1} + \left[\frac{U_{j+1,k}}{\Delta X} + \frac{V_{j+1,k}}{\Delta Y} - \frac{V_{T\ j+1,k}}{\Delta Y} \right] C_{j+1,k} +$$

$$\left[\frac{\rho^*_{j+1,k+1}\ V_{T\ j+1,k+1}}{\rho^*_{j+1,k}\ (\Delta Y)} \right] C_{j+1,k+1} = \frac{U_{j+1,k}}{\Delta X} C_{j,k} \qquad (3.8)$$

Cold Wall ($V < 0$) :

$$\left[\frac{U_{j+1,k}}{\Delta X} - \frac{V_{j+1,k}}{\Delta Y} - \frac{V_{T\ j+1,k}}{\Delta Y} \right] C_{j+1,k} + \left[\frac{V_{j+1,k}}{\Delta Y} + \frac{\rho^*_{j+1,k+1}}{\rho^*_{j+1,k}} \frac{V_{T\ j+1,k+1}}{(\Delta Y)} \right] C_{j+1,k+1} = \frac{U_{j+1,k}}{\Delta X} C_{j,k} \qquad (3.9)$$

This discretisation of species mass conservation equation is first order accurate in ΔX and ΔY. It should be emphasized here that V does not necessary change sign at all X-locations.

3.2 Method of Solution

The computation of the values of U, V, T and C is carried by "marching", starting from the stagnation point (X=0). The equations (3.1) to (3.3) are linearised to facilitate the search for the solution. This is done by taking the values of ρ^*, μ^*, and k_g^* (as the case may be) at the location (j+1) equal to the corresponding values at the location (j). In addition, the coefficients $U_{j+1,k}$ and $V_{j+1,k}$ (due to the non-linear terms) in Equation (3.2) is replaced by their computed values in the previous iteration, indicated by the primed quantities in Equation (3.2). The linearised tridiagonal set of momentum equation is solved iteratively using the discretised continuity equation (3.1) to update V at the location (j+1).

Once the values of U and V have been computed at the (j+1) location, the discretised energy equation (3.3) written for k = 1(1)n becomes a tridiagonal set of n linear equations

that can be easily solved for n unknown values of T at the location (j+1).

The temperature values computed at the (j+1) location are substituted in constitutive equations (3.5) to (3.7) to obtain n values of ρ^*, μ^*, and k_g^* at (j+1) location. The n unknown values of V_T at this location (j+1) can now be obtained using the recent computed values of ρ^*, μ^*, and k_g^* at the location (j+1) using equation (3.4).

The solution of the discretised equation (3.8) or (3.9) (depending whether V is positive or negative) can be obtained by using the computed values of U, V, ρ^* and V_T at the (j+1) location. In the case of positive V, Equation (3.8) is selected as the discretised concentration equation. However, this equation can not be solved at k=0, in which case Equation (3.9) (multiplied by a minus sign to preserve diagonal positiveness) has to be used for this point. This procedure yields a tridiagonal set of (n+1) linear equations for the (n+1) unknown values of C at the (j+1) location. In the case of negative V, Equation (3.9) written for k=0(1)n leads to a bidiagonal set of (n+1) linear equations for the (n+1) unknown values of C.

3.3 Computational Details

The velocity, temperature and concentration boundary layer thicknesses increase as we move along the surface of the cylinder away from the stagnation point. Thus, the three boundary layer widths are adjusted separately, in the computation, while marching in the X-direction. This is done by increasing the number of mesh points, n, in the Y-direction,

at each X-location. The value of n is chosen so as to ensure that there are at least 3 grid points where $U \approx U_s$, $T \approx 1$, and $C \approx 1$. This is to ensure that the computation indeed spans all three boundary layers.

The step size X is increased systematically after marching certain number of steps in the X-direction. This has been done to improve computational efficiency. Very small ΔX (of the order of 10^{-5}) is chosen while starting from the stagnation point. This value is almost doubled at an interval of about 10 marching steps. However, beyond X=0.1, the same ΔX is used for increasingly large number of steps. Thus, in the span of X from 0 (stagnation point) to 1.60 (far away from the stagnation point), twelve different step sizes are used for computation. Table 3.1 gives the value of ΔX used and the number of steps marched with each ΔX.

Because central differencing is employed in the Y- direction, it is preferable to keep ΔY uniform to preserve second order accuracy. But then the number of simultaneous equations to be solved increases excessively because the steep gradients near the wall restrict ΔY to a very small value. This increases computer time, storage space and also round-off error. A practical solution to this problem is to employ a fine mesh near the cylinder surface and a relatively coarse mesh away from it. Accordingly, a self- adaptive grid scheme is used along the Y-direction. This needs modification of the discretised equations (see Hornbeck,1973;Appendix) at locations where the mesh size in the Y-direction changes. The minimum value of ΔY

Table 3.1 : Marching Pattern along X-direction

Serial No.	ΔX	Number of steps marched	Final X value
1.	0.00001	20	0.0002
2.	0.00002	10	0.0004
3.	0.00005	12	0.0010
4.	0.00010	10	0.0020
5.	0.00020	10	0.0040
6.	0.00050	12	0.0100
7.	0.00100	10	0.0200
8.	0.00200	10	0.0400
9.	0.00500	12	0.1000
10.	0.01000	25	0.3500
11.	0.01000	105	1.4000
12.	0.01000	20	1.6000

is set at 0.005 and the maximum at 0 05. Self-adaptive grid generation technique (see section 3.4) distributes values of ΔY within this range. This range of ΔY was chosen, after numerical experimentation, to optimise the calculations with respect to computational speed and accuracy

3.4 Self-Adaptive Grid Scheme

A number of grid generation techniques are in use for the solution of the boundary layer equations. The aims of an adaptive grid scheme is to optimise the distribution of grid points while controlling grid skewness. The grid must remain as orthogonal as possible since excessive skewness causes increased truncation errors. Most of the adaptive grid methods essentially attempt to equidistribute some positive weight function, $\omega(Y)$, of the solution over the field. That is,

$$\int_{Y_k}^{Y_{k+1}} \omega(Y)\, dY = \text{constant} \qquad (3\ 10)$$

for an one-dimensional problem. In discrete form, Equation (3.10) may be written as

$$\Delta Y_k\, \omega_k = \text{constant}, \qquad (3.11)$$

where ΔY_k is the grid interval, $(Y_{k+1}-Y_k)$ and ω_k is the weight function (assumed to be constant over the interval).

The self-adaptive grid scheme employed for the present computation is essentially the same as that suggested by Nakahashi and Deiwert (1986,1987). This method redistributes the

is set at 0.005 and the maximum at 0.05. Self-adaptive grid generation technique (see section 3.4) distributes values of ΔY within this range. This range of ΔY was chosen, after numerical experimentation, to optimise the calculations with respect to computational speed and accuracy

3.4 Self-Adaptive Grid Scheme

A number of grid generation techniques are in use for the solution of the boundary layer equations The aims of an adaptive grid scheme is to optimise the distribution of grid points while controlling grid skewness. The grid must remain as orthogonal as possible since excessive skewness causes increased truncation errors. Most of the adaptive grid methods essentially attempt to equidistribute some positive weight function, $\omega(Y)$, of the solution over the field. That is,

$$\int_{Y_k}^{Y_{k+1}} \omega(Y)\, dY = \text{constant} \qquad (3\ 10)$$

for an one-dimensional problem. In discrete form, Equation (3.10) may be written as

$$\Delta Y_k\ \omega_k = \text{constant}, \qquad (3.11)$$

where ΔY_k is the grid interval, $(Y_{k+1}-Y_k)$ and ω_k is the weight function (assumed to be constant over the interval).

The self-adaptive grid scheme employed for the present computation is essentially the same as that suggested by Nakahashi and Deiwert (1986,1987). This method redistributes the

grid points optimally, reducing the overall solution error. In addition it controls the orthogonality and smoothness of the grid points. A deterministic expression for the weight function ω_k, has been suggested which provides minimum empiricism as well as a good control of the parameters to the user. As suggested by Nakahashi and Deiwert (1987), the expression for weight function, ω_k chosen to be

$$\omega_k = 1 + A \bar{f}_k^B , \tag{3.12}$$

where $$\bar{f}_k = \frac{f_k - f_{min}}{f_{max} - f_{min}} . \tag{3.13}$$

When the constant A is zero, the grid points will be equally spaced. The quantity f_k is the non-negative driving function based on the solution of the problem. This f_k is usually taken to be the gradient of the flow solution over the n grid intervals. The quantities f_k and ω_k are assumed to be constant over each grid interval. Where A and B are positive constants. The grid spacing is obtained by

$$\Delta Y_k = \frac{\ell}{\omega_k \sum_{J=1}^{n} 1/\omega_J} \tag{3.14}$$

where f_{max} and f_{min} are the maximum and minimum values of f_k respectively and ℓ is the length of the line in physical space, and n is the total number of grid intervals. The constant A controls the ratio of the maximum to the minimum grid spacing. This ratio is initially specified. Thus the constant A in Equation (3.12) is given by ΔY_{max} and ΔY_{min} as

$$A = \frac{\Delta Y_{max}}{\Delta Y_{min}} - 1 \tag{3.15}$$

The constant B in Equation (3.12) is chosen such that the minimum grid spacing $\text{Min}|\Delta Y_k|$ is equal to the specified ΔY_{min}, and this can be achieved by solving the equation

$$\text{Min}|\Delta Y_k| = \Delta Y_{min} \tag{3.16}$$

The Newton - Raphson method can be used to solve Equation (3.16) starting from a first guess B^o, by the iteration relation

$$B^{m+1} = B^m + \Delta B^m, \tag{3.17}$$

where

$$\Delta B^m = \frac{\text{Min}|\Delta Y_k| - \Delta Y_{min}}{\frac{\partial \text{Min}|\Delta Y_k|}{\partial B}}, \tag{3.18}$$

and B^m represents the m^{th} guess of B. The quantity $\frac{\partial \text{Min}|\Delta Y_k|}{\partial B}$ can be evaluated using Equations (3.12) and (3.14) as

$$\frac{\partial \text{Min}|\Delta Y_k|}{\partial B} = A \sum_{J=1}^{n} \left(\frac{\Delta Y_k^2 \omega_k}{\ell \omega_J} \right) \bar{f}_J^B \ln \bar{f}_j, \tag{3.19}$$

where ω_k and ΔY_k correspond to $\text{Min}|\Delta Y_k|$. The function f_k, is interpolated on the new grid resulting from Equation (3.14) with the new value of B, and the whole process is repeated till a reasonably low value of $|\Delta B|$ is achieved.

A FORTRAN subroutine based on the above method controls the grid self-adaptation in the Y-direction. This subroutine is called at prespecified X-locations. The function f_k can

be any of the Y-gradients of U, T or C. However, for the present computation, the Y-gradient of U is chosen as it generally has the steepest slope. The minimum value of ΔY is set at 0.005 and the maximum at 0.05.

3.5 Validation of Computer Code

In order to validate the computer code used, the flow past a flat plate at zero incidence with zero pressure gradient and of constant properties was computed. The results obtained are compared with the Blasius solution for the flat plate. These comparisons are depicted in Figures (3.1) and (3.2). These two plots correspond to two different streamwise positions. Even at X = 0.01 (i.e. very close to the stagnation point) the two results are close to each other. The result obtained by computation matches verywellwith the Blasius solution at X = 1.57.

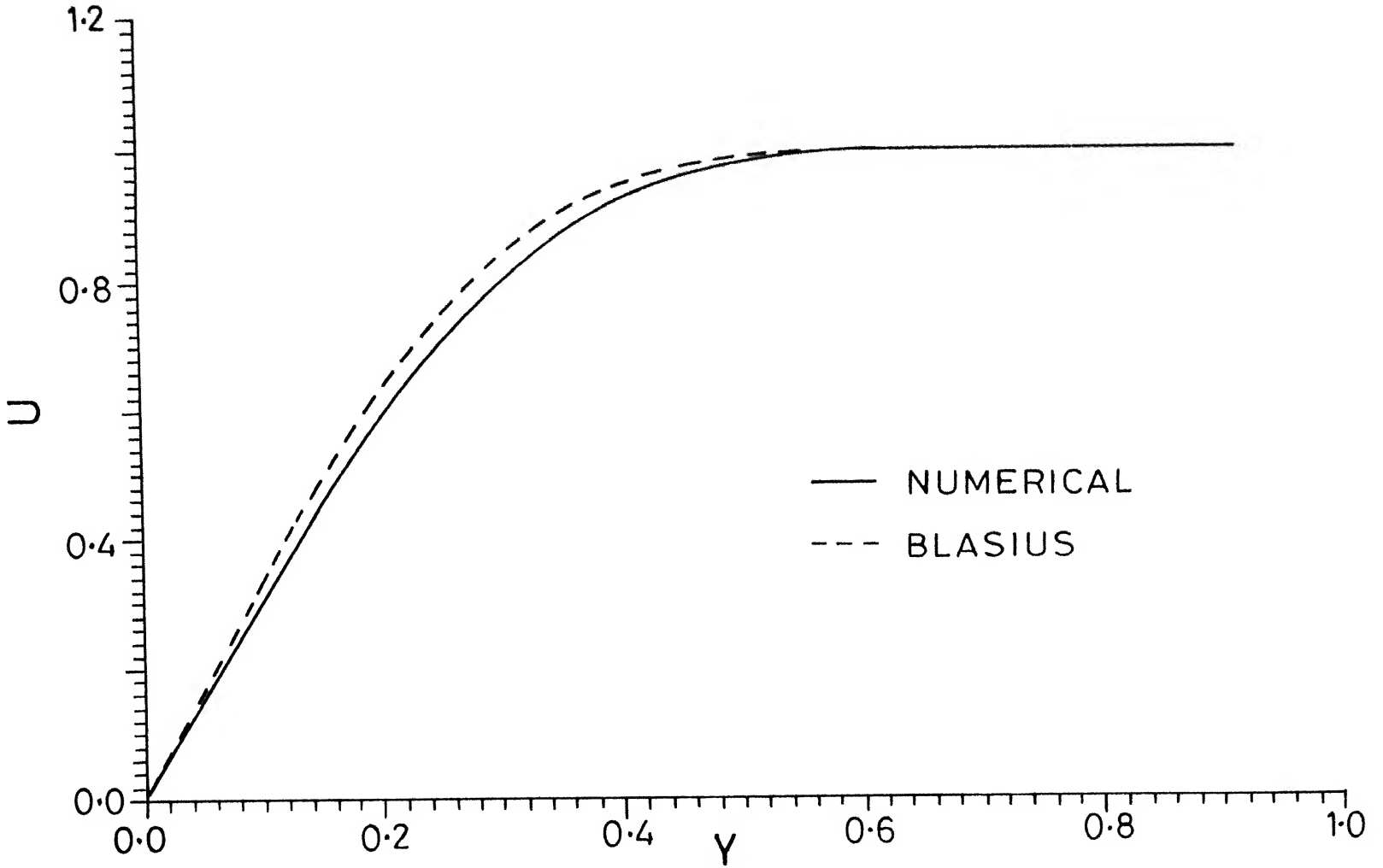

Figure 3·1 Validation of Computer Code Using Blasius Solution for a Flat Plate at X=0·01

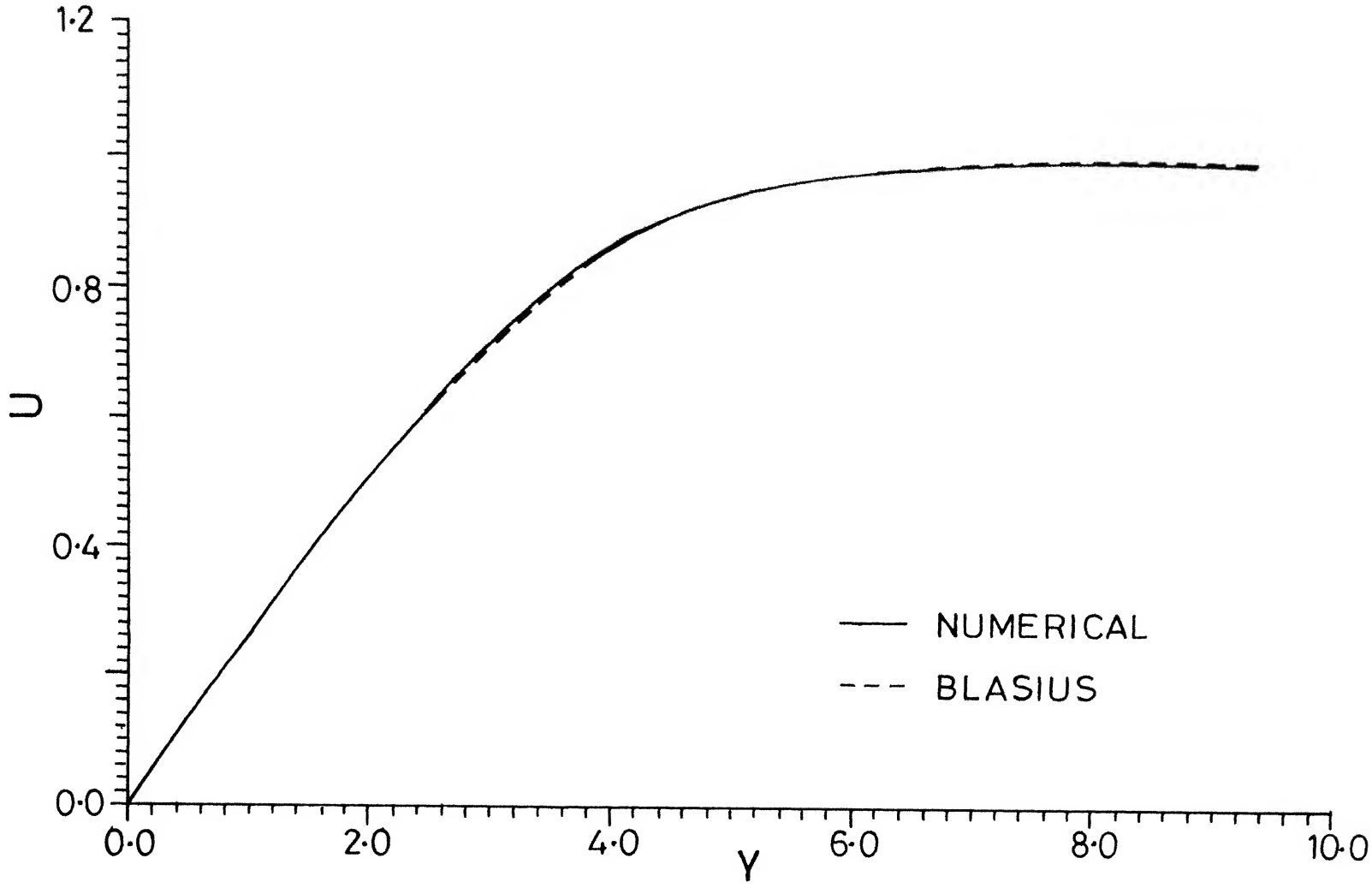

Figure 3·2 Validation of Computer Code Using Blasius Solution for a Flat Plate at X=1·57

CHAPTER 4

RESULTS AND DISCUSSION

The computer code developed and tested for the flat plate has been used to calculate the thermophoretic flow past a cold circular cylinder. Using the theoretically obtained distribution given by Equation (2.13), results are presented for a range of values of Mach number, wall temperature and thermophoretic coefficient. Special emphasis is given to the results obtained by the consideration of variable thermophysical properties. The velocity, temperature and particle concentration profiles in the boundary layer are shown in Figures 4.1 to 4.11 for $P_r = 0.7$ at various angular locations on the cylinder. A comparison between the distributions obtained with constant properties and variable properties is illustrated in every case. These profiles are shown versus the nondimensional normal distance Y, at different locations along the cylinder surface.

4.1 Hydrodynamic and Thermal Boundary Layers

The hydrodynamic and thermal boundary layers over a circular cylinder have been investigated extensively by various researchers (cf. Schlichting, 1979 and White, 1974). These results for velocity and temperature boundary layers presented here for the sake of comparison and completeness.

4.1.1 Longitudinal Velocity Profiles

The dimensionless longitudinal velocity (U/U_s) profiles for variable properties at various locations (ϕ) on

the cylinder are shown in Figure 4.1 These profiles seem to be in agreement with profiles shown in literature. Velocity distribution obtained for the constant properties case, at ϕ = 60° is presented in Figure 4.2, along with the corresponding profile for the variable properties case at the same location. The two velocity profiles are considerably different from each other. Notably, the profile for the variable properties flow has a steeper gradient compared to that of constant properties profile.

4.1.2 Transverse Velocity Profile

Figure 4.3 shows the transverse velocity profile at different X-locations for the variable properties case (Tw = 0.25, M_∞ = 0.3). It is noted that the transverse velocity component is negative over a considerable portion of the cylinder surface (upto ϕ = 70°). The effect of variable properties on the transverse velocity distribution has been illustrated in Figure 4.4, again for Tw = 0.25, M_∞ = 0.3. It appears that the assumption of constant properties leads to significant differences in the calculation of V at Tw = 0.25.

4.1.3 Normalised Temperature Profiles

Figure 4.5 shows the normalised temperature distribution in the thermal boundary layer for the variable properties case and an isothermal wall condition (Tw = 0.25). This plot indicates that the temperature gradient for ϕ = 1° is greater than that at ϕ = 90°, as expected.

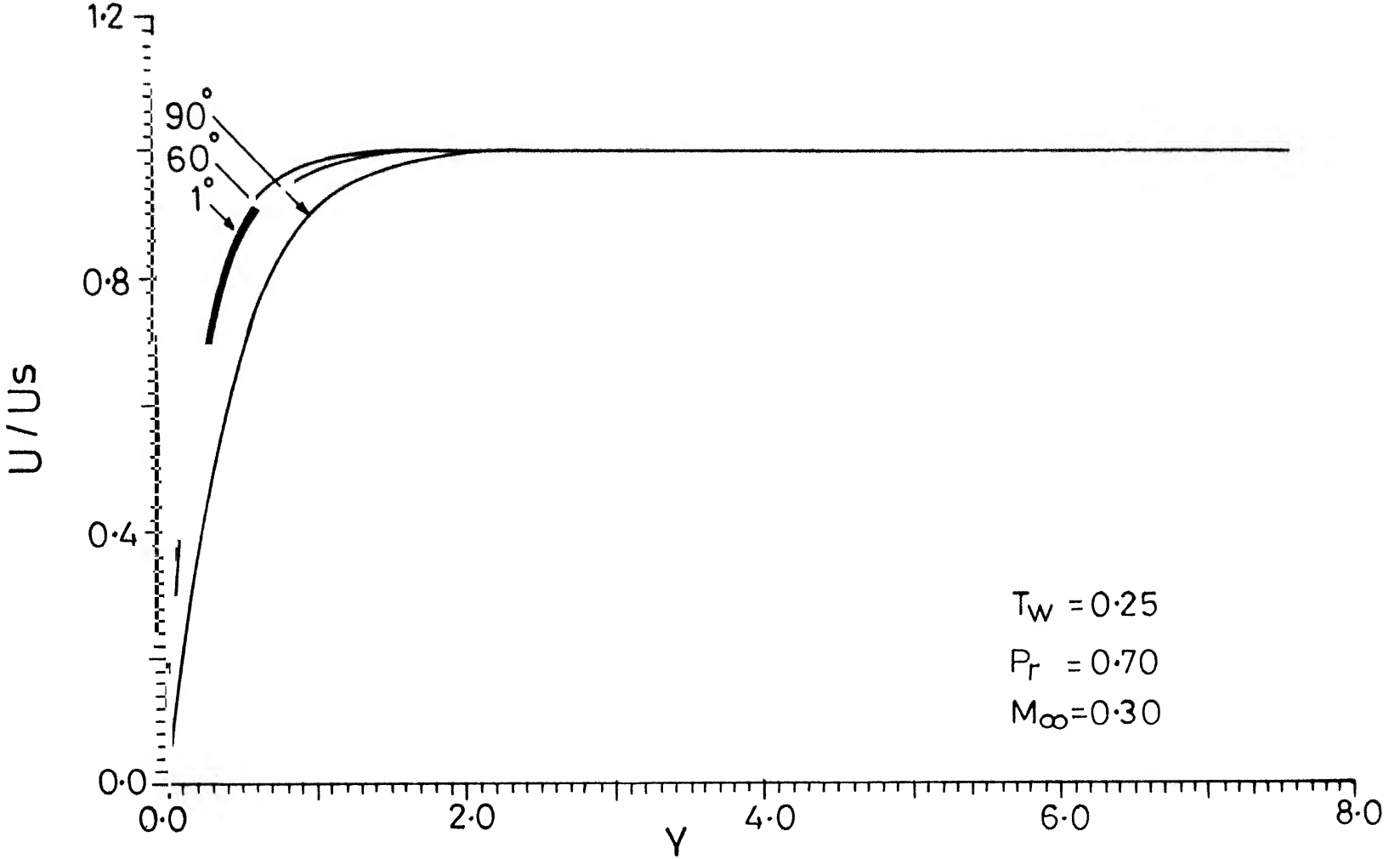

Figure 4·1 Longitudinal Velocity Distribution in the Boundary Layer on a Circular Cylinder at Different X-Locations

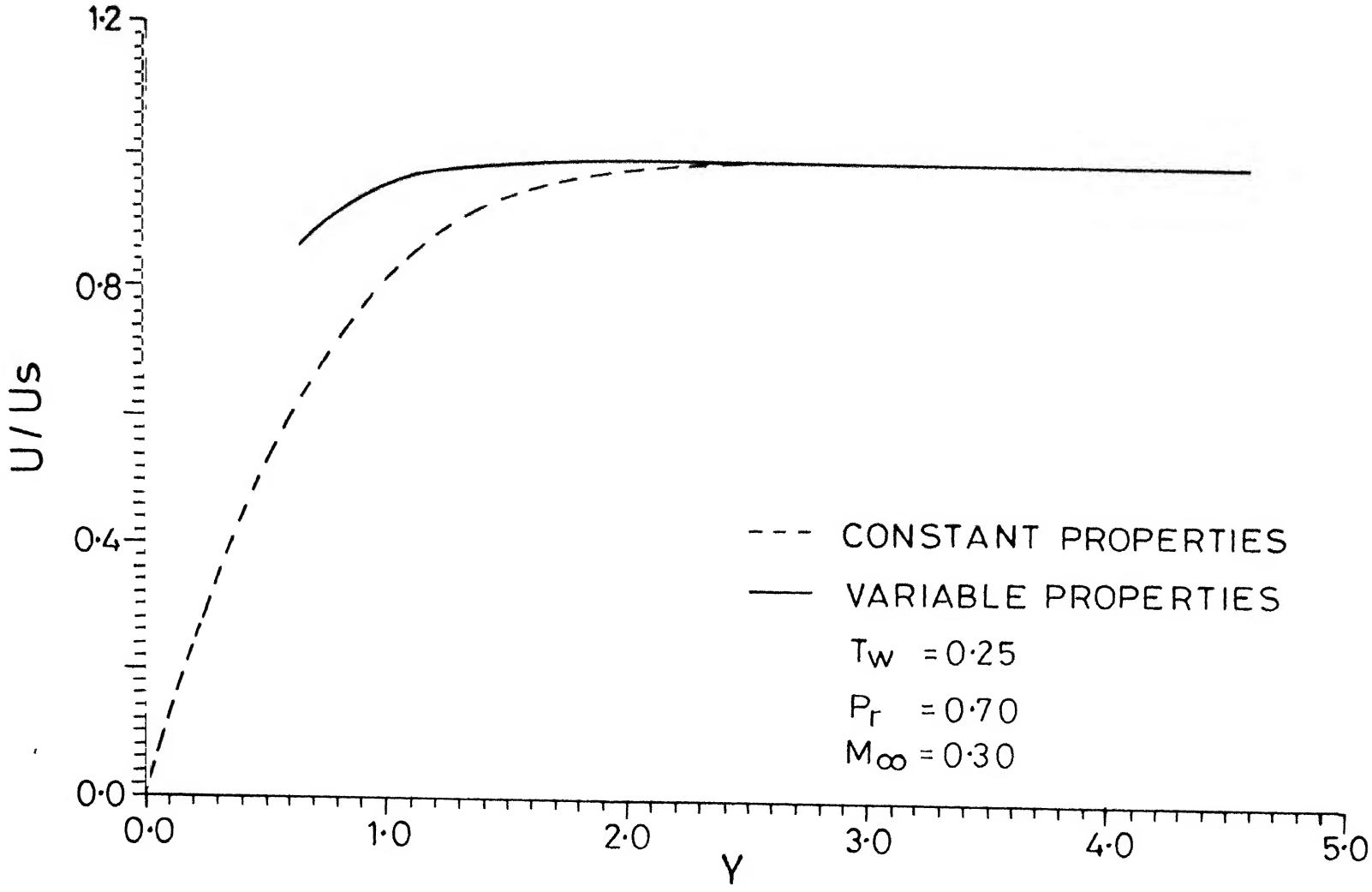

Figure 4·2 Effect of Properties Variation on the Longitudinal Velocity Distribution for Flow past a Cold Circular Cylinder ($\phi = 60^\circ$)

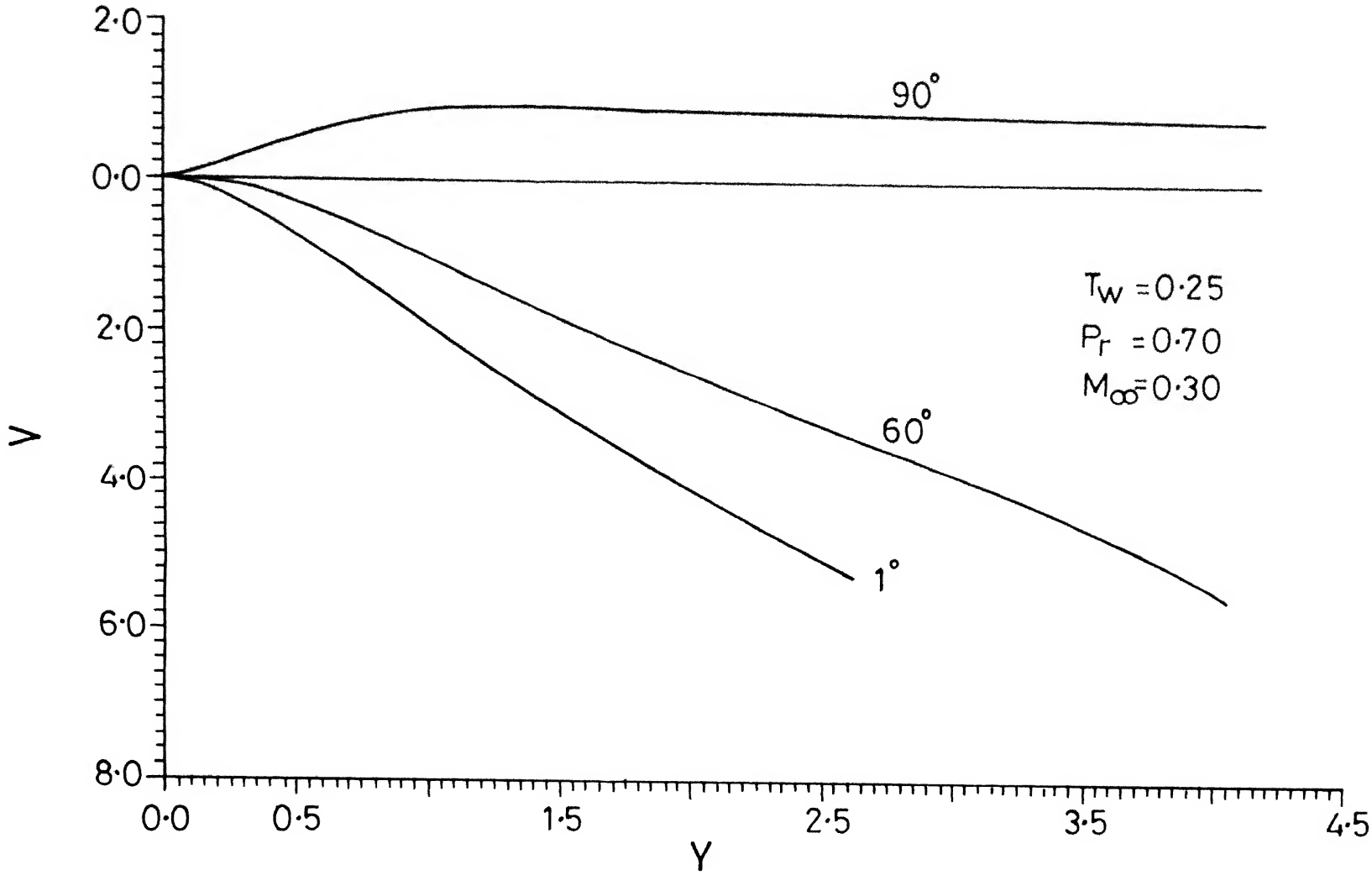

Figure 4·3 Transverse Velocity Distribution in the Boundary Layer on a Circular Cylinder at Different X-Locations

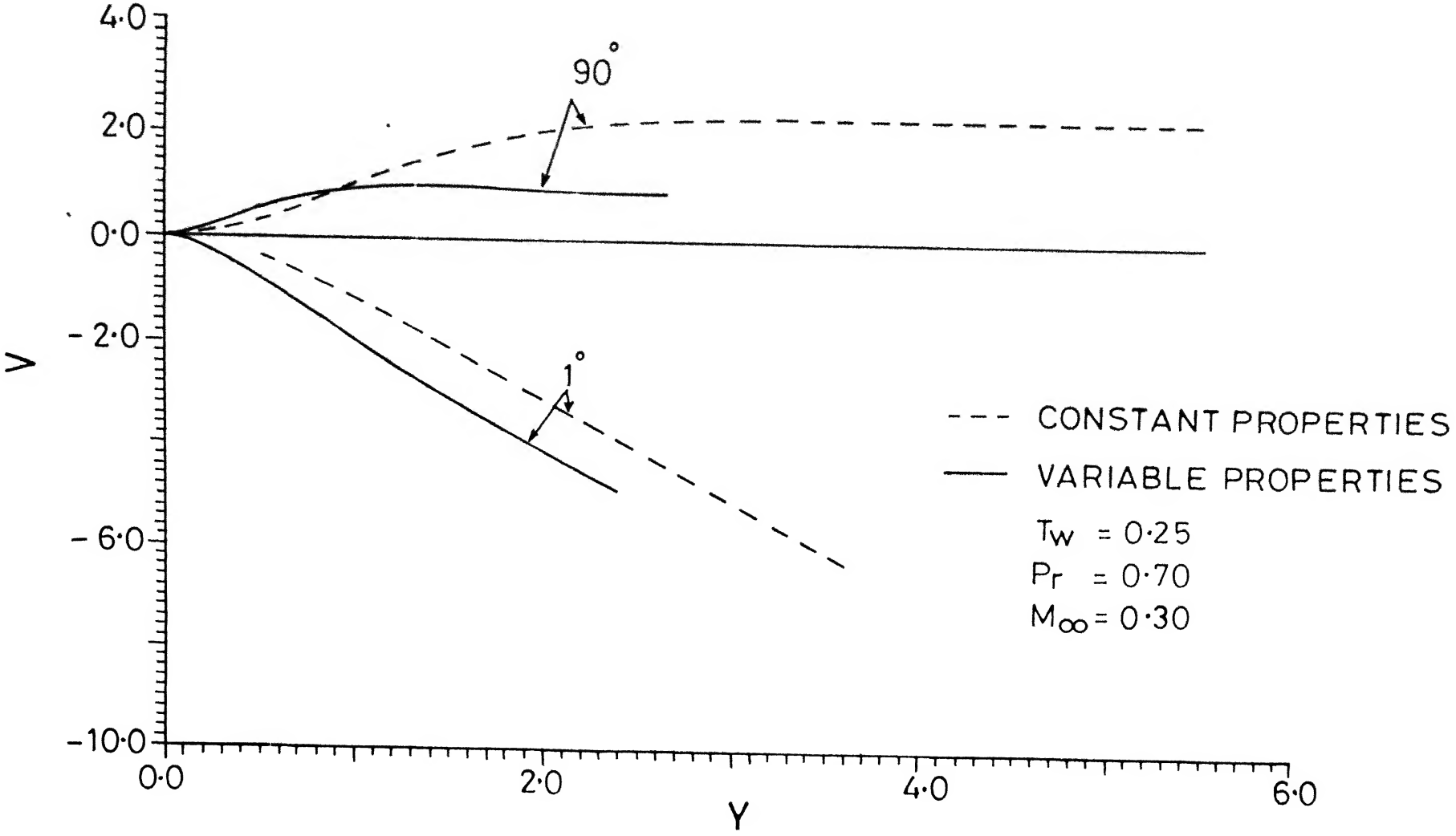

Figure 4·4 Effect of Properties Variation on the Transverse Velocity Distribution for Flow past a Circular Cylinder

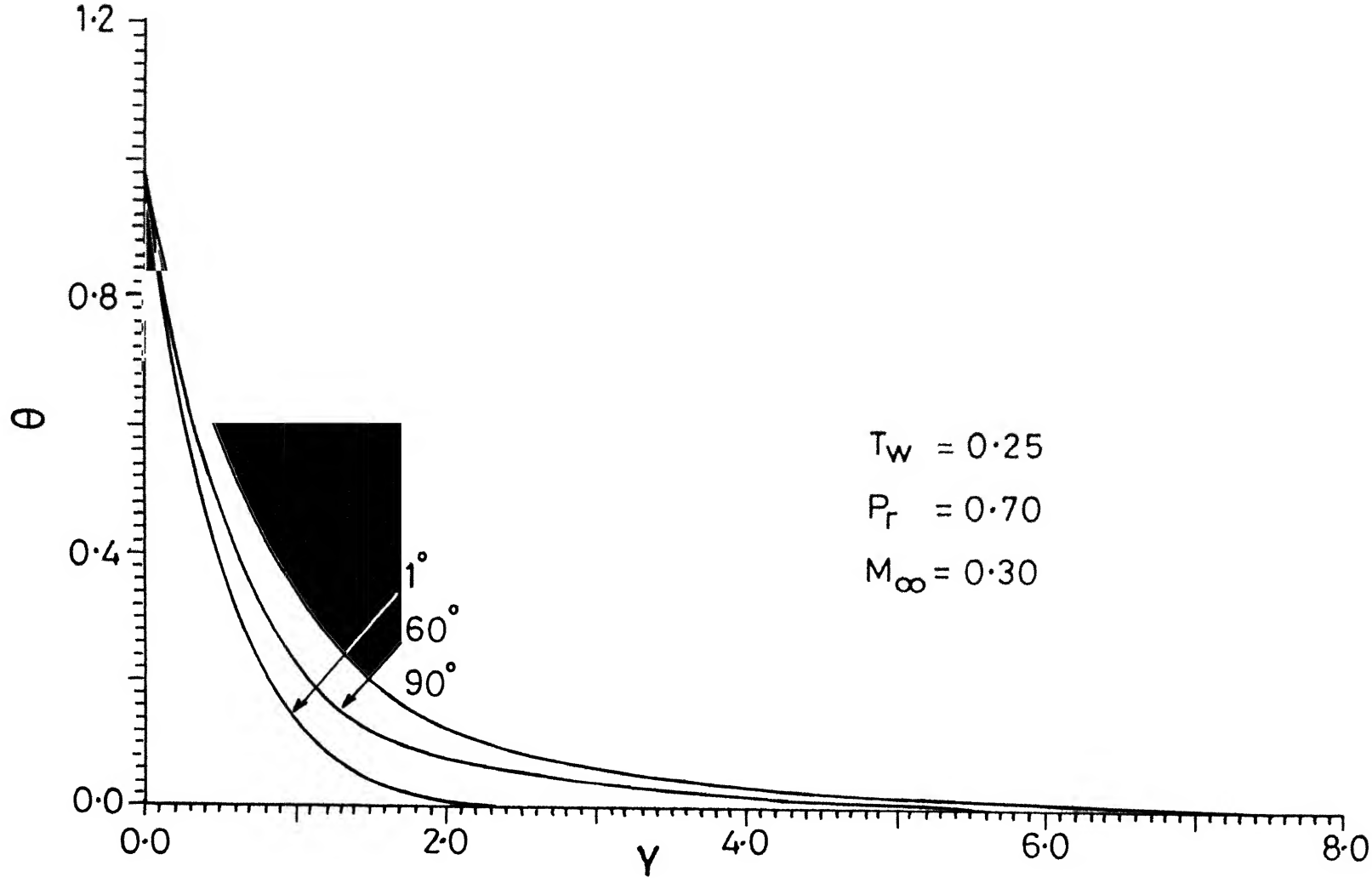

Figure 4·5 Normalised Temperature Distribution in the Boundary Layer on a Circular Cylinder at Different X-Locations

The effect of properties variation on the normalised temperature distribution is depicted in Figure 4.6. Once again the profiles drawn for the constant properties case are quite different from that of the variable properties case for Tw = 0.25.

The effect of Mach number on the normalised temperature profile is illustrated in Figure 4.7. It is noted that for a small change in the value of M_∞, the temperature profile does not alter appreciably. However, when M_∞ is increased from 0.2 to 0.5 the temperature profile is modified to a great extent. It may be noticed that the M_∞ = 0.5 profile has a less steep gradient than the lower Mach number profiles. One could expect that at higher Mach numbers the increased viscous dissipation would lead to higher temperature gradients. However, Gokoglu and Rosner have shown that even at M_∞ = 0.6, viscous dissipation hardly plays any role for Tw < 0.6 (cf. Jayaraj, 1988). Figure 4.6 is plotted for Tw = 0.25; therefore viscous dissipation can be assumed to have negligible effect in this case. Thus the profiles shown in the figure are probably influenced by the thermophysical properties variation at the various Mach numbers. However, we have not investigated this conjuncture in greater depth.

4.2 Concentration Boundary Layer

4.2.1 Particle Concentration Profiles

Figure 4.8 shows the particle concentration profiles at various X-locations. Although the profiles are similar,

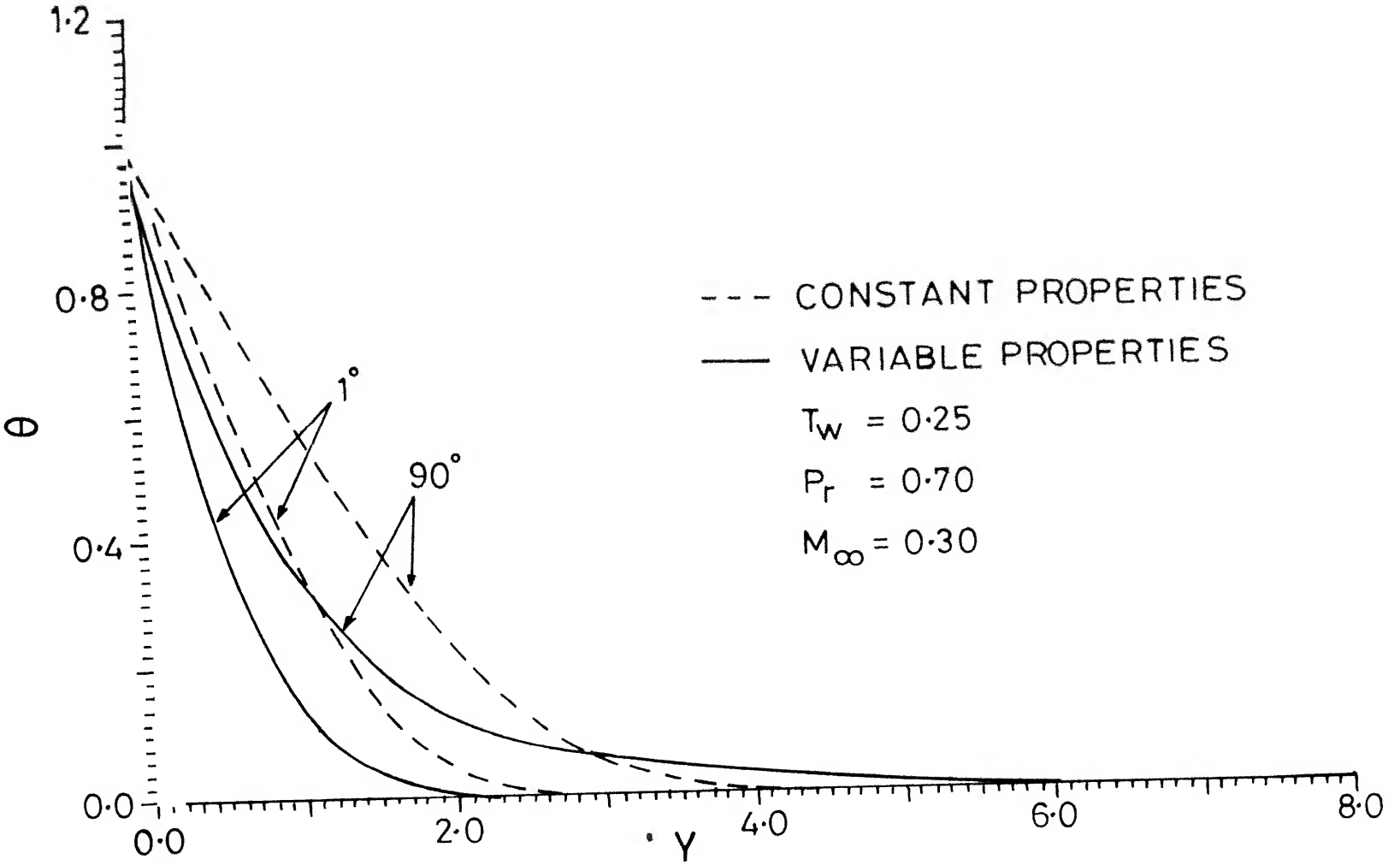

Figure 4·6 Effect of Properties Variation on the Normalised Temperature Distribution for Flow past a Circular Cylinder

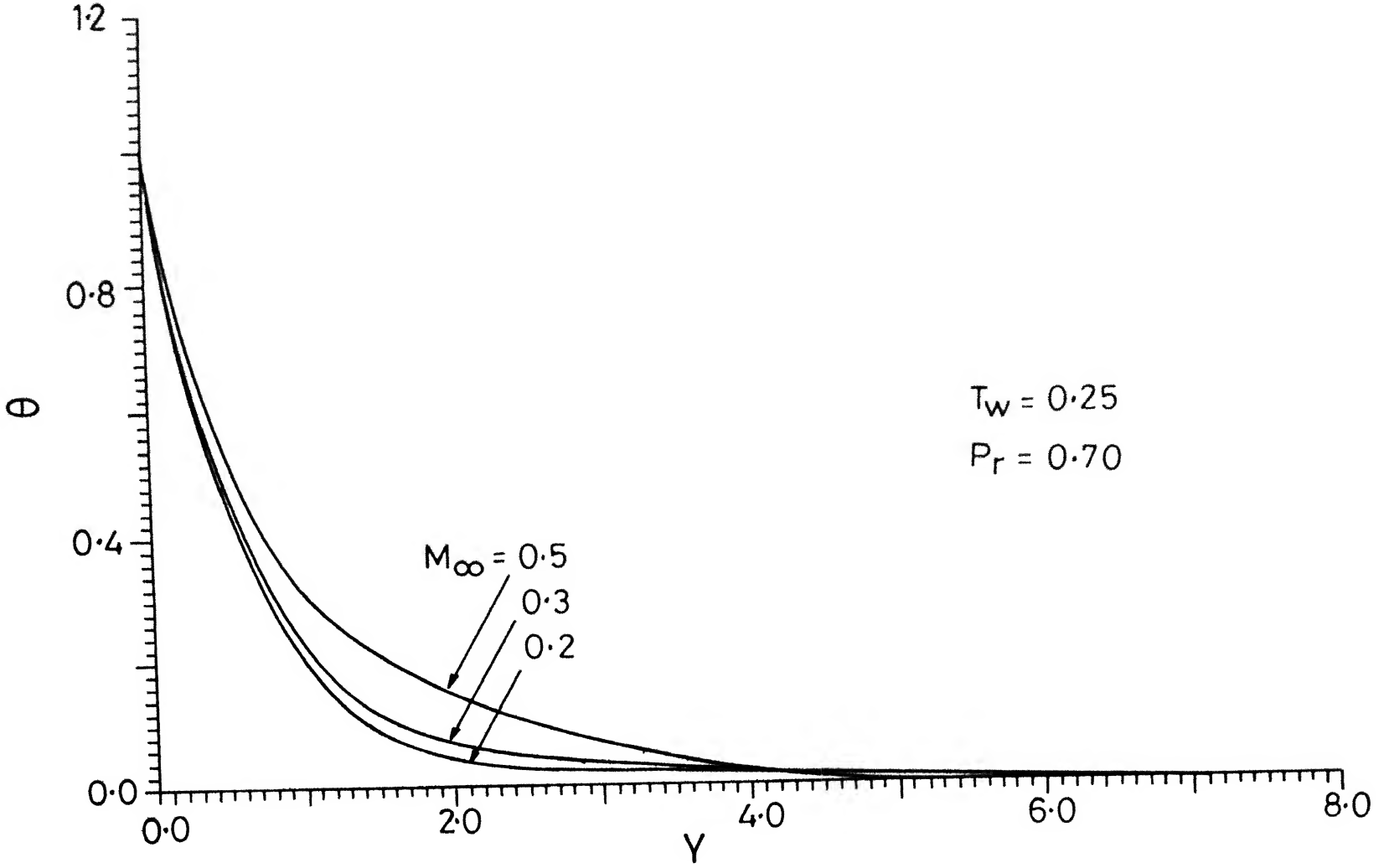

Figure 4·7 Effect of Mach Number on the Normalised Temperature Profiles for Flow past a Cold Circular Cylinder (ϕ=60°)

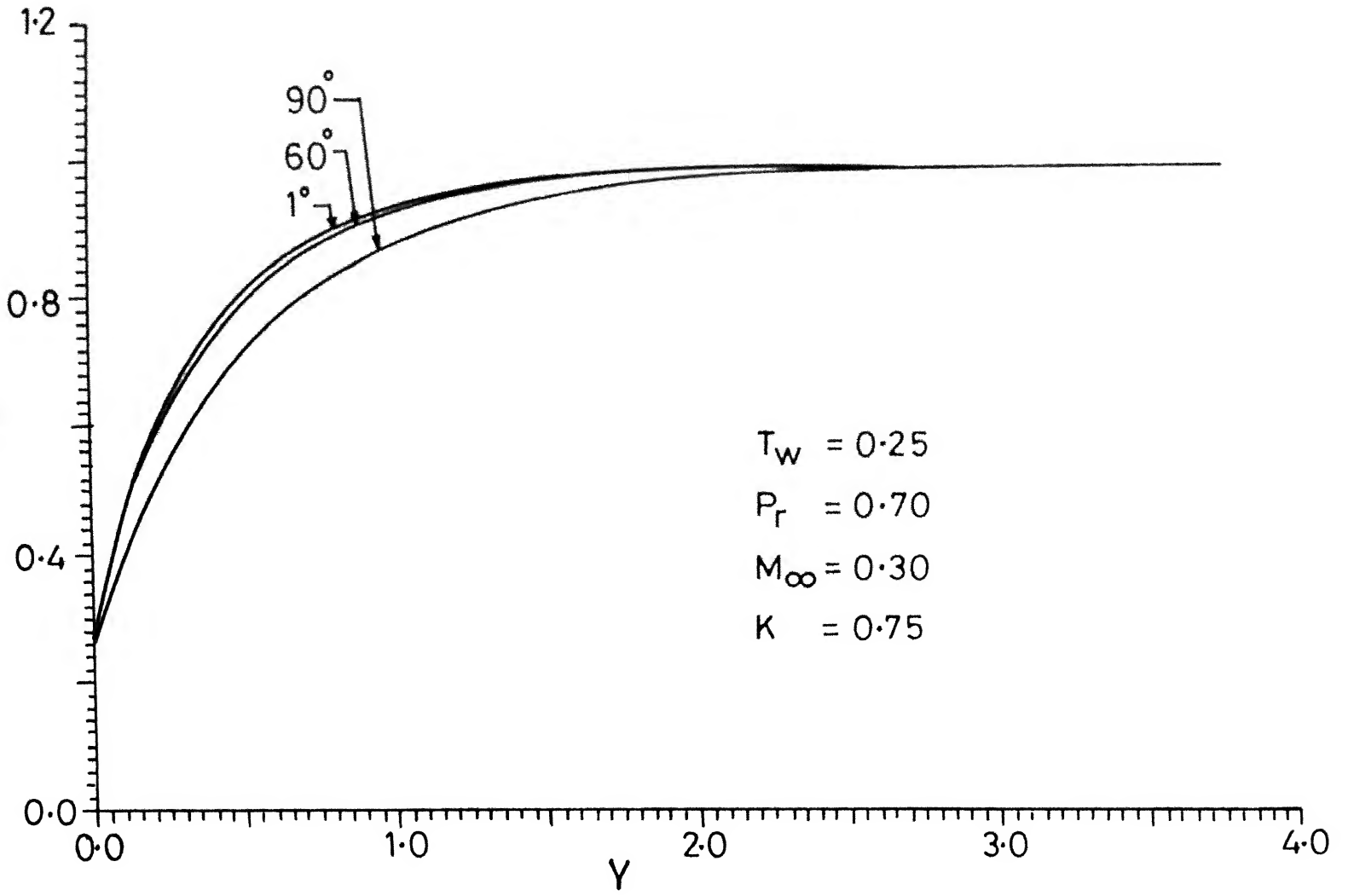

Figure 4·8 Particle Concentration Profiles over a Cold Circular Cylinder at Different X-Locations

they are not identical, i.e., they do vary along the surface of the cylinder. However, the particle concentrations at the wall are essentially constant throughout the entire range of X. This remarkable fact has already been noticed for the case of constant property (Batchelor and Shen, 1985, Epstein et al, 1985 and Jayaraj, 1988) and for variable density flows (Goren, 1977 and Shen, 1989).

Figure 4.9 demonstrates that the concentration profiles change significantly upon making the constant property assumption. In these computations too, the wall concentration is essentially constant and independent of X. However the constant property assumption over-estimates the wall concentration by about 20% for this case (Tw = 0.25, P_r = 0.7, M_∞ = 0.7, K = 0.75).

Table 4.1 gives a comparison of C_w values obtained in the present study with those obtained by Shen (1989).

Figure 4.10 displays the particle concentration profiles at a single X-position (ϕ = 60°) for flows of Mach numbers 0.2, 0.3 and 0.5. It is clear that the Mach number has a noticeable, but not pronounced, effect on the concentration profile

Figure 4.11 demonstrates the effect of wall temperature on the particle concentration profile at a particular X-location (ϕ = 60°). The figure shows that the profiles become less steep, and the particle concentration at the wall increases, with increasing wall temperature. This is similar to the results already obtained for the constant property case by

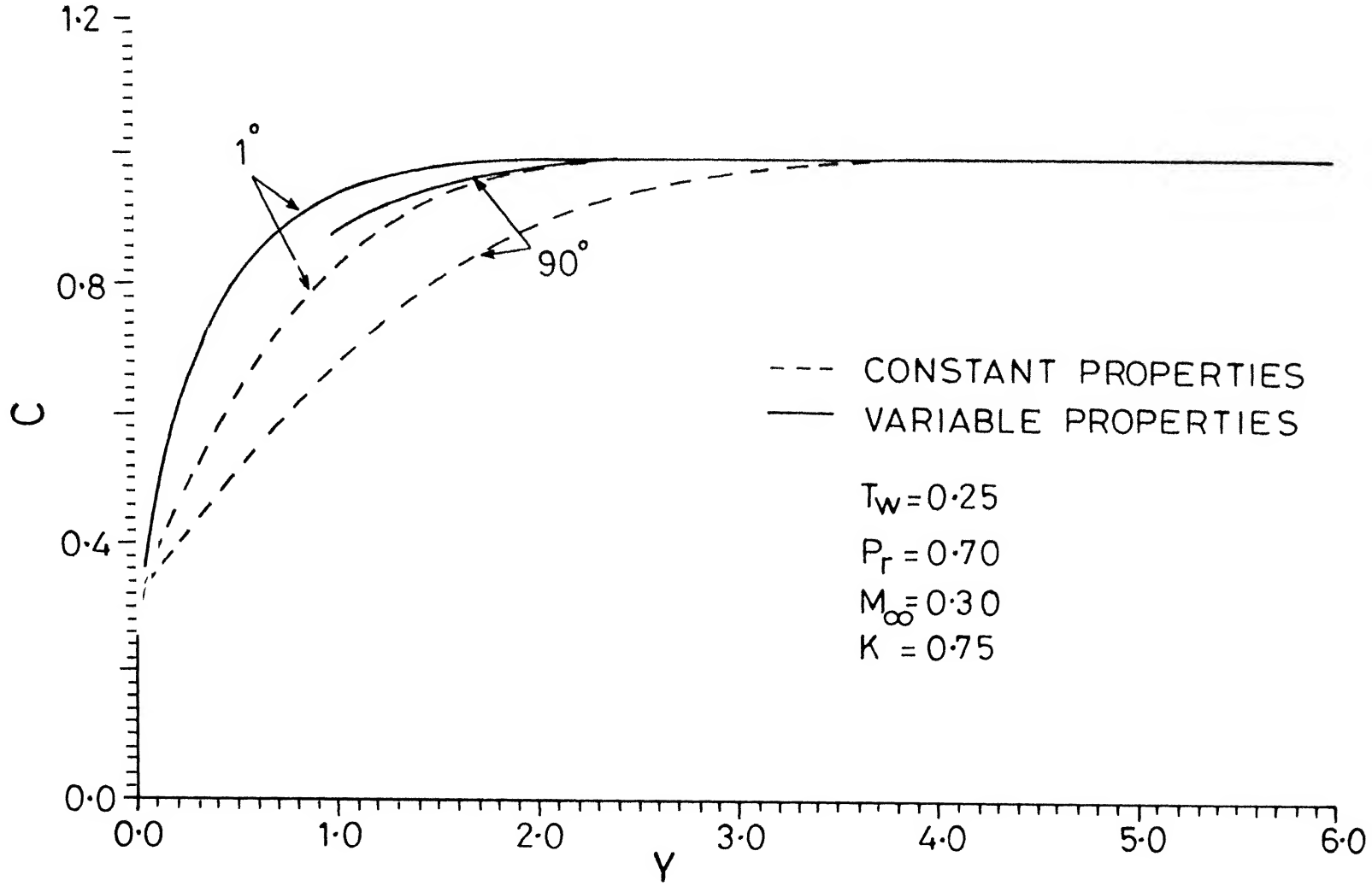

Figure 4·9 Effect of Properties Variation on the Particle Concentration Profiles for Flow past a Cold Circular Cylinder

Table 4.1 : Values of Wall Particle Concentration near the Stagnation Point on a Cold Circular Cylinder (P_r = 0.72)

P_r.K	T_w					
	0.20		0.50		0.80	
	(a) $M^2_{\infty<<1}$	(b) M_∞ = 0.5	(a) $M^2_{\infty<<1}$	(b) M_∞ = 0.25	(a) $M^2_{\infty<<1}$	(b) M_∞=0.2
0.80	0.2198	0.1877	0.5336	0.5008	0.8247	0.8143
0.70	0.2320	0.1993	0.5534	0.5211	0.8377	0.8285
0.50	0.2640	0.2302	0.6015	0.5714	0.8675	0.8603
0.30	0.3152	0.2837	0.6688	0.6472	0.9034	0.9006
0.15	0.3881	0.3577	0.7474	0.7317	0.9375	0.9360

Note : Column (a) refer to result obtained by Shen (1989), and
(b) to that of present study

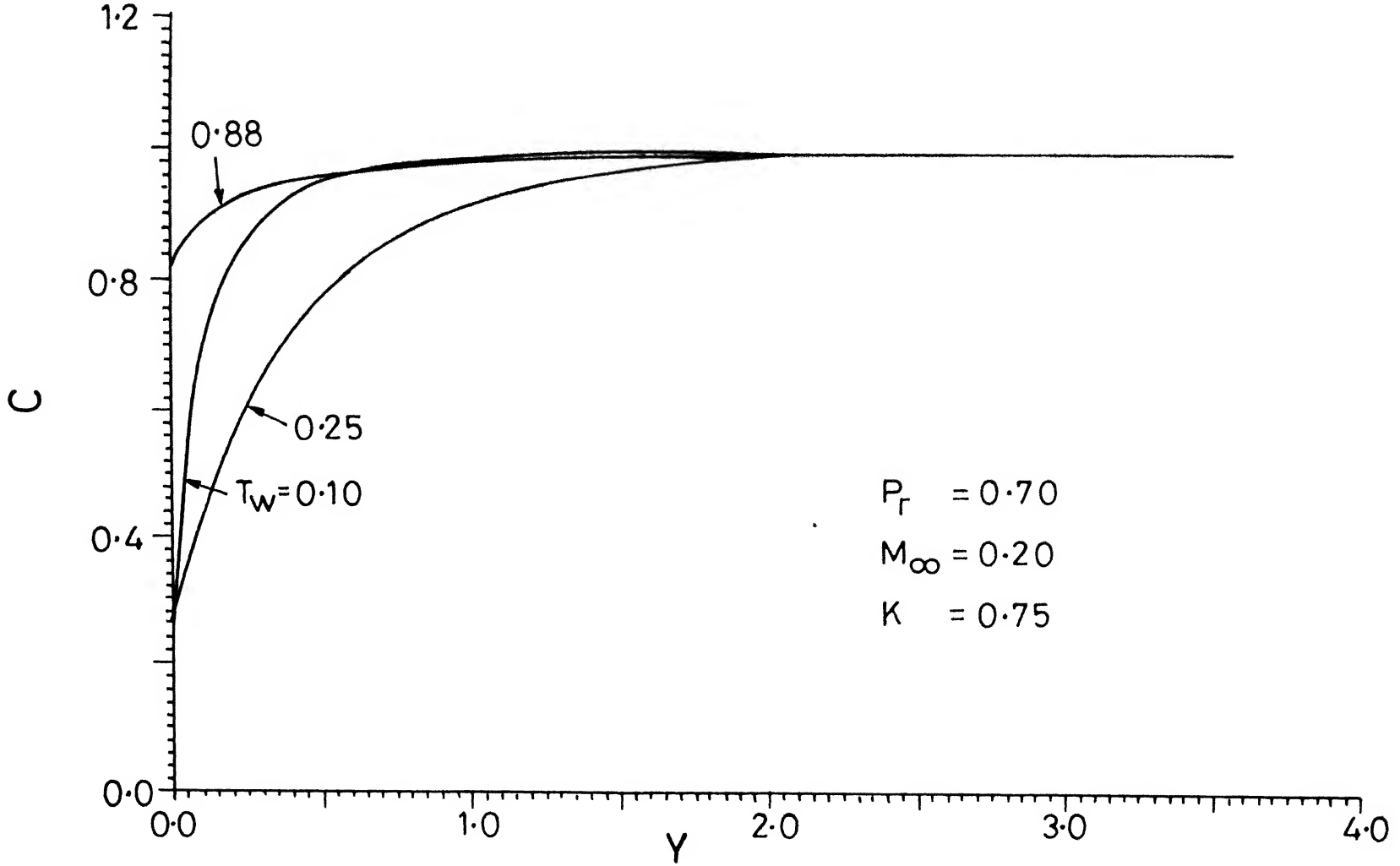

Figure 4·11 Effect of Wall Temperature on the Concentration Profiles for Flow past a Cold Circular Cylinder ($\phi = 60^\circ$)

Jayaraj (1988).

The effect of the product $P_r.K$ on the particle concentration at the wall, for different wall temperatures, is shown in Figure 4.12. This figure shows the following trends : (a) when $P_r.K$ increases, for a given wall temperature, the wall particle concentration falls and (b) for increase in wall temperature, for a given $P_r.K$, the wall concentration increases. When $P_r.K$ is zero the wall concentration is the same as the particle concentration in the free stream. These results are similar qualitatively to those obtained by Goren (1977) for forced convection over flat plate (variable density), by Epstein et al. (1985) for natural convection over a vertical flat plate for both laminar and turbulent flow (constant property), and by Shen (1989) for forced convection over a cold cylinder (variable density). Thus the relationship depicted in Figure 4.12 is remarkably universal.

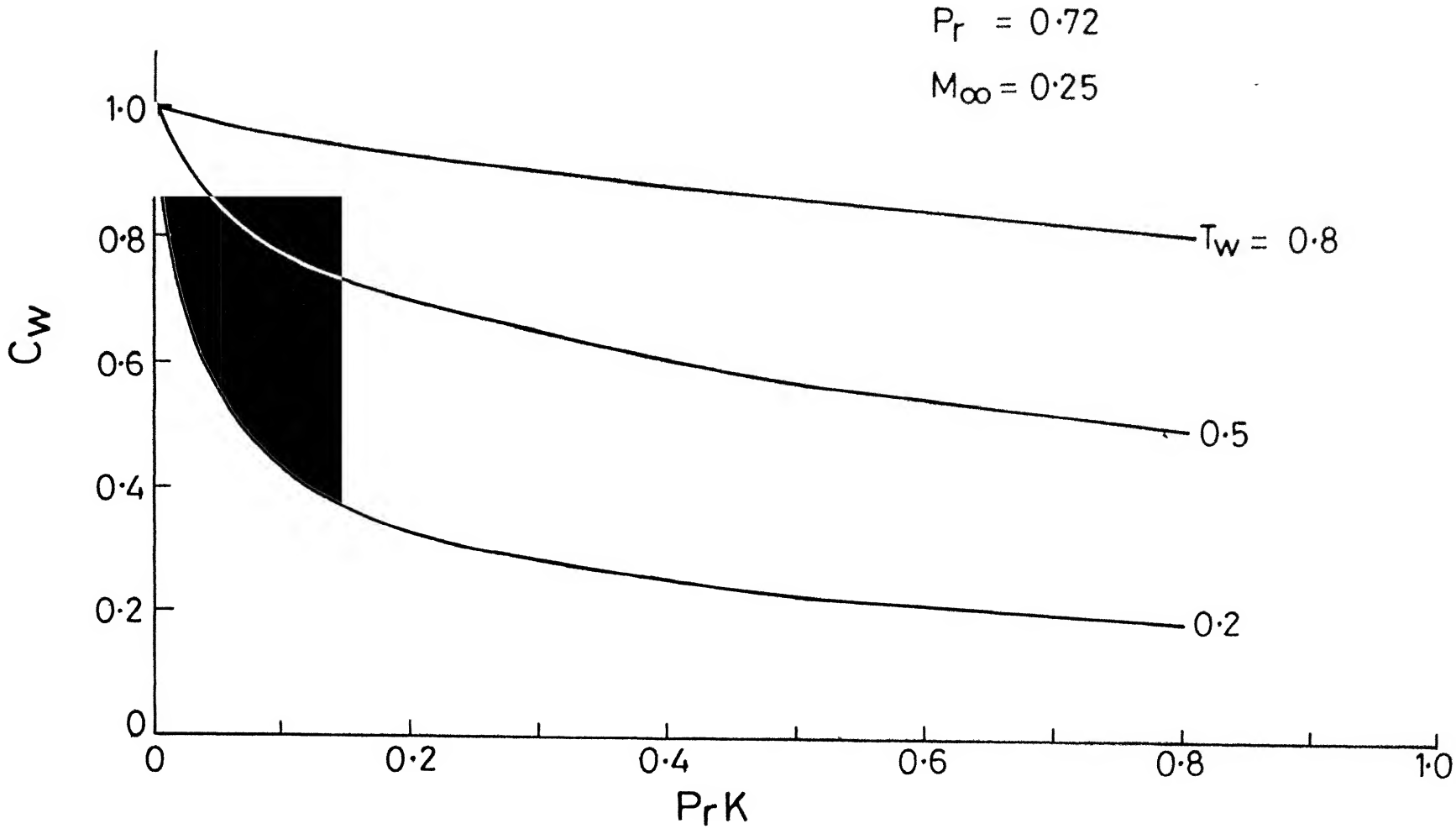

Figure 4·12 Effect of Thermophoretic Coefficient on Wall Particle Concentration near the Stagnation Point on a Cold Circular Cylinder

CHAPTER 5

C O N C L U S I O N S

Thermophoretic effects in most industrial application occur in conjunction with high temperature gradients and significant (high subsonic) Mach numbers. Although this fact is well-known, little work has been published in literature, so far, which account for the variable properties in such flows. Many researchers have concentrated on the constant properties case and low Mach numbers. Those who considered high Mach number flows have included only simple formulations (and strong assumptions) in their handling of the variable properties inherent in these flows.

This thesis has considered the variable properties flow of significant Mach number over a cold cylinder. Although the results have a qualitative similarity with the previous studies, this numerical work for a standard flow has demonstrated that the variable properties, high Mach number case is quite diferent from the constant properties, low Mach number one. In particular, the velocity, temperature and particle concentration profiles show significant differences in the two cases.

5.1 Recommendations for Further Work

The field is wide open for studies incorporating other processes which also occur in situations involving thermophoresis. For example, bouyancy effects which are particularly

strong in these situations, due to high temperature gradients, have not yet been studied in flows of engineering applications. Turbulence effects on thermophoresis can also be incorporated. No researcher has yet published any work that incorporates three-dimensional effects.....

LIST OF REFERENCES

1. Alam, M.K. and Mehrotra, S., 1987, 'Thermophoretic Deposition of Particles in Optical Fiber Preform Fabrication, ASME paper No. 87-HT-6, 24th Nat. Heat. Transfer Conf., Pittsburgh, Aug. 1987.

2. Batchelor, G.K. and Shen, C., 1985, 'Thermophoretic Deposition of Particles in Gas Flowing Over Cold Surfaces', J. Colloid Interface Sci., Vol. 107, pp. 21-37.

3. Brock, J.R., 1962, 'On the Theory of Thermal Forces Acting on Aerosol Particles', J. Colloid Sci., Vol. 17, pp. 768-780.

4. Derjaguin, B.V., Rabinovich, YA.I., Storozhilova, A.I and Shcherbina, G.I., 1976, 'Measurement of the Coefficient of Thermal Slip of Gases and the Thermophoresis Velocity of Large-Size Aerosol Particles', J. Colloid Interface Sci., Vol. 57, pp. 451-461.

5. Epstein, M., Hauser, G.M., Henry, R.E., 1985, 'Thermophoretic Deposition of Particles in Natural Convection Flow From a Vertical Plate', ASME J. Heat Transfer, Vol. 107, pp. 272-276.

6. Fuchs, N.A., 1964, The Mechanics of Aerosols, Pergamon Press, New York.

7. Gokoglu, S.A. and Rosner, D.E., 1986, 'Thermophoretically Augmented Mass Transfer Rates to Solid Walls Across Laminar Boundary Layers', AIAA J., Vol. 24, pp. 172-179.

8. Goren, S.L., 1977, 'Thermophoresis of Aerosol Particles in the Laminar Boundary Layer on a Flat Plate, 'J. Colloid Interface Sci., Vol. 61, pp. 77-85.

9. Green, H.L. and Lane, W.R., 1964, Particulate Clouds : Dusts, Smokes and Mists, 2nd Ed., E. and F.N. Spon Ltd., London.

10. Homsy, G.M., Geyling, F.T., and Walker, K.L., 1981, 'Blasius Series for Thermophoretic Deposition of Small Particles', J. Colloid Interface Sci., Vol. 83, pp. 495-501.

11. Hornbeck, R.W., 1973, Numerical Marching Techniques for Fluid Flows with Heat Transfer, SP-297, NASA, Washington, D.C.

12. Jayaraj, S., 1988, 'Thermophoresis of Aerosol Particles in Two-Dimensional Laminar Flow, Ph.D. Dissertation, Dept. of Mechanical Engineering, I.I.T. KANPUR.

13. Kennard, E.H., 1938, Kinetic Theory of Gases, McGraw-Hill, New York.

14. Nakahashi, K. and Deiwert, G.S., 1986, 'Three Dimensional Adaptive Grid Method, 'AIAA J., Vol. 24, pp. 948-954.

15. Nakahashi, K. and Deiwert, G.S.,1987, 'Self-Adaptive Grid Method with Application to Airfoil Flows',AIAA J., Vol. 25, pp. 513-520.

16. Roache, P.J., 1982, Computational Fluid Dynamics, 2nd Ed., Hermosa Publishers, Albuquerque.

17. Schlichting, H., 1979, Boundary Layer Theory,, 7th Ed., McGraw-Hill, New York.

18. Schreier, S., 1982, Compressible Flow, John Wiley & Sons, New York.

19. Shen, C., 1989, 'Thermophoretic Deposition of Particles Onto Cold Surfaces of Bodies in Two-Dimensional and Axisymmetric Flows', J. Colloid Interface Sci., Vol. 127, pp. 104-115.

20. Simpkins, P.G., Greenberg-Kosinski, S. and Macchesney, J.B., 1979, 'Thermophoresis : The Mass Transfer Mechanism in Modified Chemical Vapor Deposition', J. Appl. Phys., Vol. 50, pp. 5676-5681.

21. Talbot, L., Cheng, R.K., Schefer, R.W. and Willis, D.R., 1980, 'Thermophoresis of Particles in a Heated Boundary Layer', J. Fluid Mech., Vol. 101, pp. 737-758.

22. Walker, K.L., Homsy, G.M. and Geyling, F.T , 1979, 'Thermophoretic Deposition of Small Particles in Laminar Tube Flow', J. Colloid Interface Sci., Vol. 69, pp. 138-147.

23. Walker, K.L., Geyling, F.T., and Nagel, S.R., 1980', Thermophoretic Deposition of Small Particles in the Modified Chemical Vapor Deposition (MCVD) Process', J. Amer. Ceram. Soc., Vol. 63, pp. 552-558.

24. White, F.M., 1974, Viscous Fluid Flow, McGraw-Hill, New York.

ME-1980-M JIL